PROTON MAGNETIC RESONANCE IN PARAMAGNETIC AND ANTIFERROMAGNETIC SINGLE CRYSTALS OF $CoCl_2 \cdot 6H_2O$

by

Erich Sawatzky

B.Sc., University of British Columbia, 1958.

A thesis submitted in partial fulfilment of the requirements for the degree of

Master of Science

in the Department

of

Physics

We accept this thesis as conforming to the required standard

The University of British Columbia,

April, 1960

In presenting this thesis in partial fulfilment of the requirements for an advanced degree at the University of British Columbia, I agree that the Library shall make it freely available for reference and study. I further agree that permission for extensive copying of this thesis for scholarly purposes may be granted by the Head of my Department or by his representatives. It is understood that copying or publication of this thesis for financial gain shall not be allowed without my written permission.

Department of Physics

The University of British Columbia,
Vancouver 8, Canada.

Date 13 April, 1960.

Abstract

Standard radio-frequency nuclear resonance spectroscopy techniques have been applied to study the fine structure of the proton magnetic resonance absorption line in single crystals of $CoCl_2 \cdot 6H_2O$. Cobaltous Chloride is a paramagnetic crystal at high temperatures and becomes antiferromagnetic at about 2.29°K. The position and number of lines strongly depend on temperature and on the direction of the externally applied magnetic field. Fewer lines than the theoretical number of twenty-four were always observed.

At room temperature the proton resonance at 12 Mc/sec. in a field of 2.82 K gauss consists of a single line about six gauss wide. A splitting of this line into a maximum of six components has been observed at liquid helium temperature. The maximum overall separation at 4.2°K is about 110 gauss. For each direction of the externally applied magnetic field the separation between the lines increases with decreasing temperature.

The transition temperature is measured and effects due to short-range order above the transition are observed.

Theoretical formulae for the positions of the component lines are developed by considering the two-proton spin system within a water molecule of hydration immersed in the homogeneous external field $\vec{H}_o$ and the inhomogeneous time-

averaged field of the cobalt ions.

Measurements in the antiferromagnetic state have been partially completed.

Table of Contents

List of Illustrations

Acknowledgements

The work described in this thesis has been supported in part by research grants to Dr. M. Bloom and Dr. G.M. Volkoff from the National Research Council of Canada and through the award of a National Research Council Studentship (1959-60).

To Dr. M. Bloom, who suggested and supervised this research, I wish to express my sincere appreciation for his constant interest, many illuminating discussions, and for his invaluable help in interpreting the results.

I also wish to express my appreciation to Dr. G.M. Volkoff for critically reading the manuscript of this thesis.

My thanks are also due to Mr. W. Morrison, who constructed the magnet support.

Chapter 1

Introduction

The nuclear magnetic resonance technique provides a powerful method of studying the interactions between atomic nuclei and their magnetic environment both at high and low temperatures. The work described in this thesis represents a preliminary survey of the proton magnetic resonance in single crystals of $CoCl_2 \cdot 6H_2O$ in the paramagnetic and anti-ferromagnetic phases of this substance. Results obtained here shall serve as a guide for more detailed investigations of hydrated cobaltous chloride planned for the near future.

Chapter 2 of this thesis is a summary of the theory underlying the experimental work to be described and Chapter 3 is a description of the experimental apparatus. Chapter 4 is a report of the experimental observations on single crystals of $CoCl_2 \cdot 6H_2O$ in external magnetic fields up to 3200 gauss and at temperatures down to 1.52°K. The experimental data so obtained yield information on both the crystal structure and the electronic wave functions of the atoms comprising the crystal, and bring out some of the difficulties encountered in paramagnetic crystals with a relatively large number of water molecules of hydration.

In general, if a sample containing non-interacting nuclei with spin $I \neq 0$ and magnetic moment $\vec{\mu}$ is placed in a uniform magnetic field $\vec{H}_o$, the nuclei can each assume a maximum number of $2I + 1$ orientations with respect to $\vec{H}_o$. In this work only the resonance spectrum of the protons in the water molecules of hydration is studied. Since the spin of a proton is $I = \frac{1}{2}$, only two orientations are possible, giving rise to two different energy levels separated by $2\mu_p H_o$. Transitions between these energy levels may be induced by an externally applied r-f field $\vec{H}_1$ at right angles to $\vec{H}_o$ and of angular frequency $\omega_o = 2\mu_p H_o/\hbar$. The coil around the sample is part of the resonant circuit of an oscillating detector. This coil produces the desired r-f field $\vec{H}_1$, and in absorption experiments it usually also serves as the pick-up coil.

Resonance may be observed by monitoring the level of oscillation of the r-f oscillator as its frequency is varied. A dip in the level of oscillation results when transitions are induced between the nuclear Zeeman levels, since then energy is absorbed from the r-f field. As described later, this resonance absorption, though peaked at the classical Larmor frequency $\omega_o = \mu H_o/I\hbar$, occurs over a range of frequencies as indicated schematically in figure 1.

It is often convenient, for signal-to-noise considerations, to modulate the magnetic field periodically while sweeping the oscillator frequency through the resonance, and to use the method of phase sensitive detection in recording the r-f level of oscillation. With a modulation amplitude smaller than the line width the derivative of the resonance

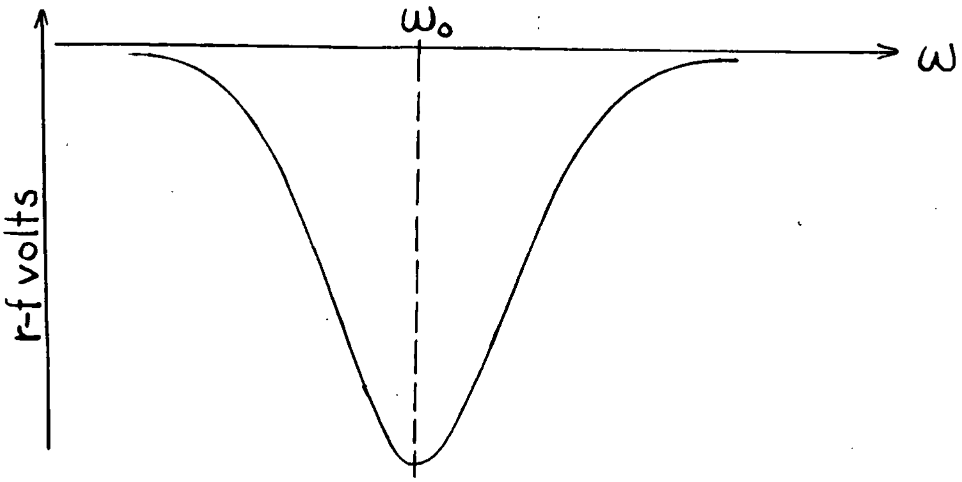

Fig. 1. Dip in level of oscillation as the frequency of the oscillator passes through the Larmor frequency ω_0.

to follow page 2

line is observed as indicated schematically in figure 2.

The simple picture of non-interacting nuclei outlined above is never strictly true. Interactions with the surrounding magnetic moments are always present, although in liquids and gases these interactions are averaged considerably, the line widths usually being determined by inhomogeneities in the externally applied magnetic field.

In the case of solids the picture changes considerably. We shall consider only crystalline solids. Here all nuclei, except for their thermal vibrations, are situated in fixed positions and each nucleus experiences in addition to the externally applied fields $\vec{H}_o$ and $\vec{H}_1$ a local magnetic field due to the neighbouring magnetic dipoles. If the crystal contains paramagnetic ions, this local field may be of the order of $|H_{local}| \simeq 1000$ gauss; the local field due to other nuclei is usually not larger than about 20 gauss. Since the nuclei and paramagnetic ions are each oriented in $2I + 1$ and $2S + 1$ different ways respectively, the field produced by the surroundings at the sites of different nuclei in a unit cell may vary between about $+ |H_{local}|$ and $- |H_{local}|$.

In the case of non-paramagnetic single crystals with only one type of nuclear magnetic moment present (those of the waters of crystallization) Pake[1] showed theoretically and observed experimentally that the proton resonance line is split into two components by the dipole-dipole interaction between the proton-pair in the water molecule.

The separation of the lines in any given observation

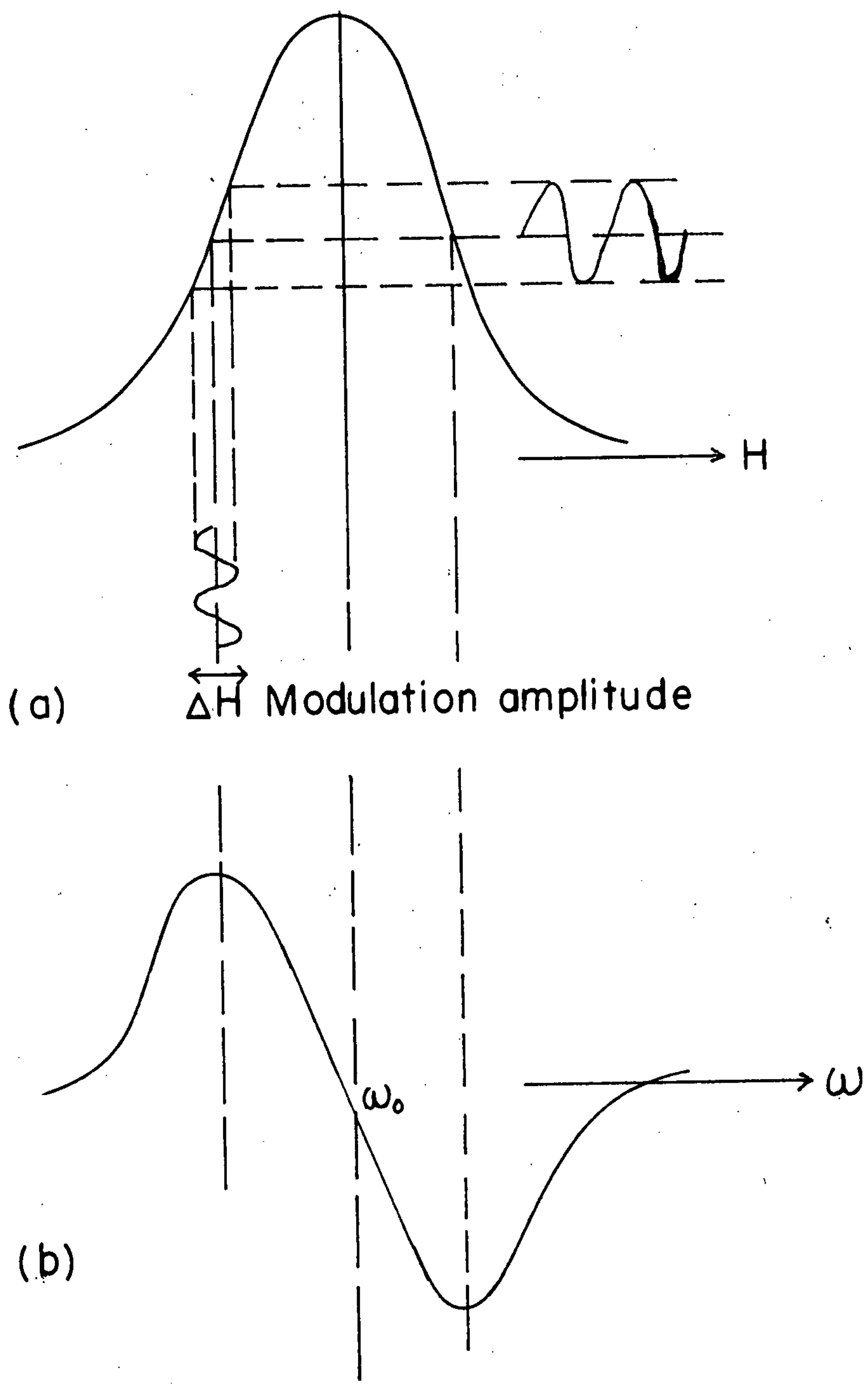

Fig. 2. Field modulation ΔH smaller than line width (a), derivative of line (b).

to follow page 3

also depends on the orientation of the crystal with respect to the external field $\vec{H}_o$. If the sample is a paramagnetic crystal, we have, in addition to the interactions between the nuclear dipoles and the external fields and between the protons themselves, the interactions between the protons and the electronic magnetic moments of the paramagnetic ions. This interaction gives rise to additional decomposition of the proton resonance line. Such fine structures of the proton magnetic resonance line were treated theoretically and observed experimentally by N. Bloembergen[2] in $CuSO_4 \cdot 5H_2O$ and by N.J. Poulis[3,4] in $CuCl_2 \cdot 2H_2O$.

When observing the proton resonance in paramagnetic crystals we would expect a very broad line because of the large magnetic interactions between the protons and the paramagnetic ions. But it can be shown[5] that if exchange forces between the magnetic ions are present, this broadening action of the magnetic ions may be considerably reduced. In the case of $CoCl_2 \cdot 6H_2O$ such exchange interactions are present and at room temperatures we observe a single line about six gauss wide. As a first approximation the temperature dependence of the resonance spectrum may be obtained from the Curie law, which states that at high temperatures the mean magnetization $\langle\mu\rangle$ of a magnetic ion in a field $\vec{H}_o$ at temperature T is given by

$$\langle\mu\rangle = \mu^2 H_o/3kT$$

where the average is over time. This mean magnetization gives rise to a time-average local field which depends strongly on the space coordinates in the crystal and on the orientation of the magnetic moments. The energy levels of the proton magnetic moments are determined by the vector sum of this local field with $\vec{H}_o$. However, in paramagnetic resonance work, the local field is usually much smaller than H_o, and we consider only the component in the direction of $\vec{H}_o$ of the local field. Thus a different total magnetic field is produced at the different sites in a unit cell, and the different protons in the unit cell have different Larmor frequencies. Assuming that H_o is constant over the sample, the local field will be the same for corresponding protons in different unit cells. Since the local field increases with decreasing temperature, the resonance line splits into a number of component lines as the temperature is lowered. Therefore, the number of components observed depends on temperature, on the number of water molecules in the unit cell and on the degree of symmetry possessed by the crystal.

The internal field at a proton due to a magnetic ion a distance r away is of order of magnitude $\langle\mu\rangle/r^3$. Since the r-dependence is an inverse cube, only the near neighbours will have any profound influence on the splitting and the shape of the lines. Taking $r = 2 \times 10^{-8}$ cm and $H_o = 3000$ gauss, the splitting at 300°K is about 1 gauss, at 78°K about 4 gauss, and at 4°K about 70 gauss. We therefore do not expect any resolution of the resonance line at room temperature.

Theory predicts that $CoCl_2 \cdot 6H_2O$ has a possible maximum number of 24 component lines each of which should be several gauss wide, so that we cannot expect a complete resolution in a field of 3000 gauss even at liquid helium temperatures. The maximum number of 24 lines was never observed. At 4.2°K only six lines were found.

In order to calculate the positions of the lines as a function of crystal parameters, temperature, and the external field H_o, degenerate perturbation theory is applied to the Hamiltonian describing the system. To simplify matters, some approximations are made, since some of the terms in the Hamiltonian are much smaller than others. These calculations are summarized in Chapter 2.

Chapter 2

Theory

This part of the thesis consists of a summary of the theory of steady state nuclear resonance spectroscopy as applied to paramagnetic crystals. Although none of it represents original work by the author, nevertheless, its inclusion is required to interpret the experimental work presented in Chapter 4.

We consider a paramagnetic crystal with one or more water molecules of hydration whose crystal structure is at least partially known. From X-ray investigations for instance, the oxygen positions can be determined, but not the proton positions. Both the proton magnetic moments with spin $I = \frac{1}{2}$ and the electronic magnetic moments of the paramagnetic ions with spin S produce local magnetic fields throughout the crystal. The magnitude and direction of this local field at any given point depend on the orientation and separation of the moments at any given time, since both moments precess about the external magnetic field $\vec{H}_o$. Thus we have a system of protons immersed in the homogeneous external field $\vec{H}_o$ and the rapidly varying inhomogeneous field produced by the paramagnetic ions. The entire Hamiltonian describing this system may be written in the form

$$(1) \qquad H = -\sum_k \beta \vec{S}_k \cdot \vec{g}_k \cdot \vec{H}_o + H_{SS} + H_{ex}{}^S + H_{SI} + H_{II} - \sum_i \gamma_i h \vec{I}_i \cdot \vec{H}_o$$

The quantities g_k and β represent the g-factor of cobalt written as a tensor and the nuclear Bohr magneton respectively. The first term in H represents the Zeeman energy of the paramagnetic ions in the external field $\vec{H}_o$, H_{SS} the magnetic interaction between the paramagnetic ions themselves, $H_{ex}{}^S$ the exchange interaction between them; H_{SI} is the magnetic interaction between the paramagnetic ions and the proton moments, H_{II} the magnetic interaction between the protons themselves, and $\sum_i \gamma_i \hbar I_i H_o$ represents the magnetic interaction between the proton moments and the external field $\vec{H}_o$. The proton magnetic moment is denoted by $\gamma \hbar \vec{I}$, where $\vec{I}$ is the spin operator and γ the gyromagnetic ratio. This notation is customary in nuclear magnetic resonance work[6] and keeps the nuclear and electron spins clearly separated. The term in equation (1) connecting the two spin systems is H_{SI} and may be written

$$(2) \qquad H_{SI} = \sum_{ik} \left\{ \frac{\gamma_i \hbar \vec{I}_i \cdot \vec{\mu}_k}{r_{ik}^3} - \frac{3\gamma_i \hbar (\vec{I}_i \cdot \vec{r}_{ik})(\vec{\mu}_k \cdot \vec{r}_{ik})}{r_{ik}^5} \right\}$$

where $\vec{\mu}_k$ is the magnetic moment of the k^{th} magnetic ion and $\vec{r}_{ik}$ is the radius vector connecting the i^{th} proton and the k^{th} ion and $r_{ik} = |\vec{r}_{ik}|$. But $\vec{\mu}_k$ varies rapidly in time due to the exchange coupling between the magnetic ions represented by $H_{ex}{}^S$. The exchange interaction causes a pair of antiparallel spins to flip simultaneously, i.e. if two spins are oriented as $\uparrow\downarrow$ and one reverses direction, the other also flips due to the exchange coupling. The exchange frequency is approximately given by $\hbar\omega_{ex} \cong kT_N$, where T_N is the Neel temperature. For $CoCl_2 \cdot 6H_2O$, $T_N \simeq 2°K$, so that $\nu_{ex} \simeq 5 \times 10^{10}$ cycles/sec. The Larmor frequency for protons in a field of 3000 gauss is 12.8 Mc/sec. so that the protons cannot follow the rapid variations of the local field due to the cobalt ions. Thus the protons see only the time-average field of the cobalt ions. We therefore can use the time average $\langle\vec{\mu}_k\rangle$ of $\vec{\mu}_k$ in equation (2). We shall also neglect the term H_{SS} compared with H_{ex}^{S}, since the exchange energy between a pair of cobalt ions is about 100 times greater than their magnetic energy. The time-average magnetization $\langle\vec{\mu}_k\rangle$ of the k^{th} cobalt ion can now be calculated in principle from the reduced Hamiltonian for the cobalt system by the diagonal sum method described by Van Vleck[7].

The effect of the time-average magnetization μ_k on the proton resonance is obtained from the Hamiltonian for the proton spin system, with $\vec{\mu}_k$ replaced by $\langle\vec{\mu}_k\rangle$ in H_{SI}. Written out in full, the proton Hamiltonian becomes:

$$(3) \qquad H_p = -\sum_i \gamma_i \hbar \vec{I}_i \cdot \vec{H}_o + \sum_{ik} \left\{ \gamma_i \hbar \left[\frac{\vec{I} \cdot \langle\vec{\mu}_k\rangle}{r_{ik}^3} - 3\, \frac{(\vec{I}_i \cdot \vec{r}_{ik})(\langle\vec{\mu}_k\rangle \cdot \vec{r}_{ik})}{r_{ik}^5} \right.\right.$$

$$+ \sum_{ij} \left\{ \frac{\gamma\hbar \vec{I}_i \vec{I}_j}{r_{ij}^3} - 3\, \frac{(\vec{I}_i \cdot \vec{r}_{ij})(\vec{I}_j \cdot \vec{r}_{ij})}{r_{ij}^5} \right\}$$

Since the dipole-dipole interaction is proportional to $\frac{1}{r_{ij}^3}$, the most important terms in the proton-proton interaction are those representing the coupling between nearest neighbours. Therefore, only interactions between the proton pair in the same water molecule are considered. The interactions with other protons and the time dependent part of the field due to the cobalt ions contribute only to the line widths of the component lines. We now have a two-proton system immersed in the homogeneous field $\vec{H}_o$ and the static inhomogeneous field of the cobalt ions. To find the position of the resonance lines, equation (3) must be solved for its eigenvalues which give the energy levels of the system. Using this Hamiltonian, N. Bloembergen[2] obtains for the energy levels to first order:

$$
\begin{aligned}
E_1 &= -\gamma\hbar\, H_o + a + d \\
E_2 &= -d + \sqrt{b^2 + d^2} \\
E_3 &= -d - \sqrt{b^2 + d^2} \\
E_4 &= +\gamma\hbar\, H_o - a + d
\end{aligned}
\tag{4}
$$

where

$$
\begin{aligned}
a &= \tfrac{1}{2}\gamma\hbar\, (H_z^1 + H_z^2) \\
b &= \tfrac{1}{2}\gamma\hbar\, (H_z^1 - H_z^2) \\
d &= -1/4\, \gamma^2\hbar^2\, (1 - 3\cos^2\theta_{12})r_{12}^{-3} \\
H_z^i &= \sum_k \langle\vec{\mu}_k\rangle\, (1 - 3\cos^2\theta_{ik})r_{ik}^{-3},\ (i = 1,\ 2)
\end{aligned}
\tag{5}
$$

and H_z^1 and H_z^2 are the z-components of the field produced by the cobald ions at protons 1 and 2 respectively when Z is chosen parallel to $\vec{H}_o$. a and b are functions of temperature by virtue of H_z^1 and H_z^2 which are calculated from H_{SI} with μ_k replaced by

$\langle\vec{\mu}_k\rangle$. The energy levels of (4) give rise to four transition frequencies as follows:

$$
(6)\qquad
\begin{aligned}
h\nu_1 &= \gamma hH_o - a + 2d + \sqrt{b^2 + d^2} \\
h\nu_2 &= \gamma hH_o - a - 2d - \sqrt{b^2 + d^2} \\
h\nu_3 &= \gamma hH_o - a + 2d - \sqrt{b^2 + d^2} \\
h\nu_4 &= \gamma hH_o - a - 2d + \sqrt{b^2 + d^2}
\end{aligned}
$$

with corresponding intensities

$$
(7)\qquad
\begin{aligned}
I_1 = I_2 &= \frac{(b-d-\sqrt{b^2+d^2})^2}{b^2+d^2-b\sqrt{b^2+d^2}} \qquad \text{and} \\
I_3 = I_4 &= \frac{(b-d+\sqrt{b^2+d^2})^2}{b^2+d^2+b\sqrt{b^2+d^2}}
\end{aligned}
$$

We thus have a maximum of four lines for each proton pair in every water molecule in the unit cell. The maximum number of proton lines in $CoCl_2 \cdot 6H_2O$ should therefore be 4 x 6 (number of H_2O molecules per formula) ÷ 2 (because of reflection symmetry of the unit cell) x 2 (number of formula units per unit cell), which gives 24 lines.

In this chapter we have followed the usual description of magnetic fields at nuclear positions in paramagnetic crystals and neglected the contribution to <u>average</u> magnetic field due to the <u>average</u> magnetization M per unit volume. If contributions of this sort are important as we later see that they are, the external field H_o which appears in this chapter should everywhere be replaced by $\vec{B} = \vec{H}_0 + (4\pi - N)\,\vec{M}$, where N, the demagnetization factor for the crystal being studied, must be calculated from the geometry of the crystal[8]. If the crystal is not an ellipsoid, $\vec{M}$ will be a function of position in the crystal and this non-uniformity will be equivalent to an inhomogeneity in the applied field in that it will also contribute to the nuclear resonance line width.

Chapter 3

Apparatus and Experimental Procedure.

A standard steady state nuclear resonance spectrometer was used for the work reported in this thesis. A block diagram of the apparatus is shown in figure 3, and photographs in figure 4.

The oscillating detector used was a slightly modified version of a circuit of Watkins and Pound[9]. The original circuit is described in detail in reference 9, and the modifications by H.H. Waterman[10] and shall not be dealt with here. The narrow band amplifier and phase sensitive detector were built and fully described by H.H. Waterman[10]. The remainder of the apparatus is standard equipment and shall not be described, except for its use in this work.

The large magnetic field $\vec{H}_o$ was supplied by an air-cooled iron-core electromagnet manufactured by Newport instruments Co., which has four inch diameter plane pole tips with adjustable air-gap. The cryostat was of such dimensions that the air-gap could not be less than 3.2 cm. With this air-gap and a field of 3000 gauss the homogeneity was measured to be about 0.3 gauss per cm. The magnet is mounted on a rotating table provided with a circular brass scale graduated in degrees and with a vernier arranged to measure the magnet orientation to one tenth of a degree. The whole support was constructed in such a way that the magnet can conveniently be rotated through 360 degrees

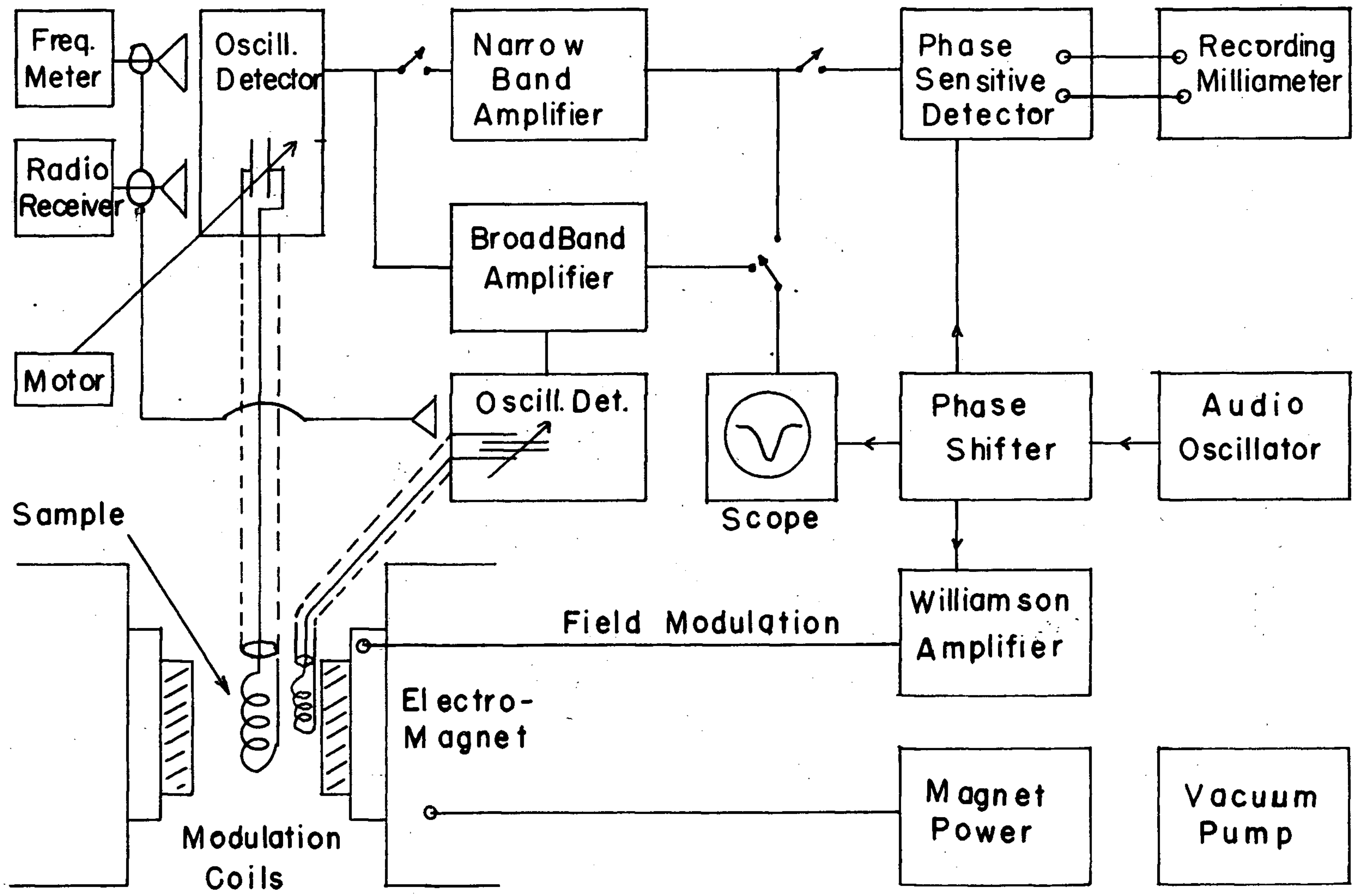

Fig. 3. BLOCK DIAGRAM OF APPARATUS.

to follow page 13

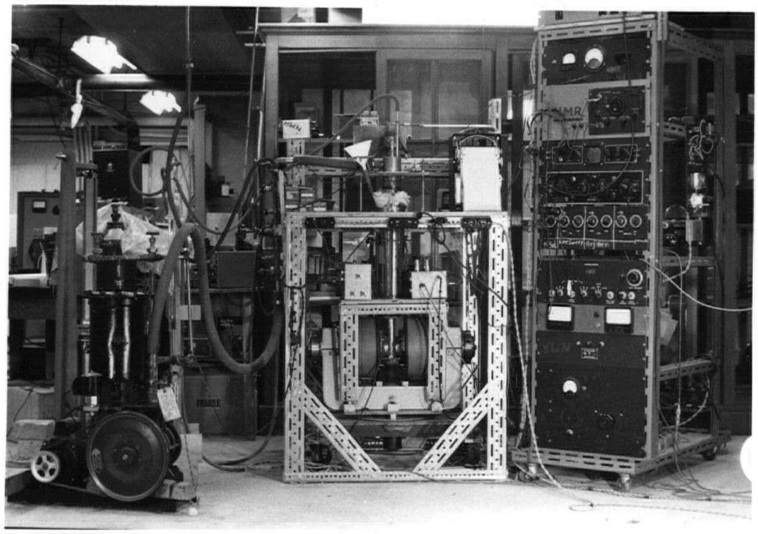

General View

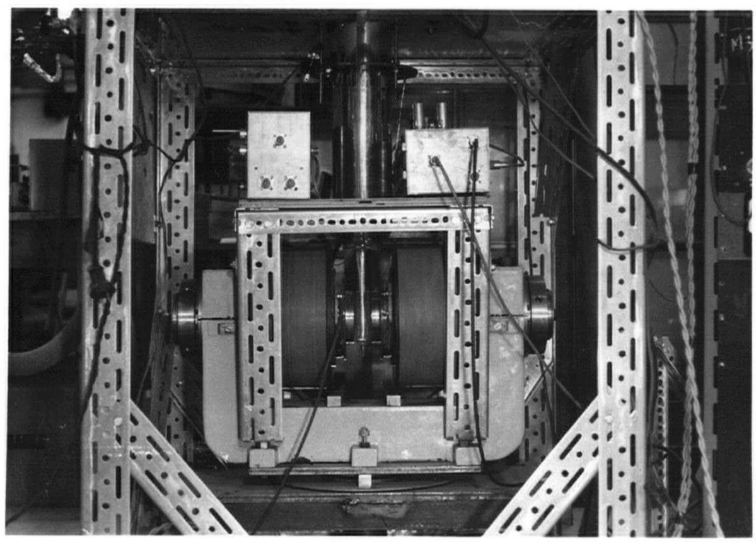

Magnet Arrangement

Figure 4

Photographs of Apparatus

to follow page 13

without interfering with the rest of the apparatus.

Cylinders about 1.5 cm long and 0.8 cm in diameter were cut from fairly large crystals, which were of the same type described by P. Groth[11]. During this operation great care was taken to make one of the crystal axes parallel to the axis of the cylinder. The preparation of the crystals proved to be a difficult task, mainly because $CoCl_2 \cdot 6H_2O$ crystals have a low melting point (86°C) and are quite brittle. Two such cylinders were cut, one with the a-axis and the other with the b-axis parallel to the cylinder axis. In each case the crystal was attached to the end of a German silver tube 1 cm in diameter and 80 cm long. The cylinders were mounted in such a way that their axes were parallel to the axis of the German silver tube. The r-f coil was wound directly on the crystal to give as high a filling factor as possible. The number of turns in the coil was chosen to give the r-f oscillator a frequency range of about 7.5 Mc/sec. (7 Mc/sec. - 14.5 Mc/sec.). When aligned, the crystal with coil and the end of the German silver tube were imbedded in "Plastic Wood" and then coated with glue to insure a permanent mount (see fig. 5). During the mounting the direction of the axis perpendicular to the cylinder axis (hence to one of the crystal axes) was marked on the brass piece at the top end of the German silver tube, so that the orientation of the crystal is known with respect to the supporting frame, and hence the magnetic field $\vec{H}_0$. The angular

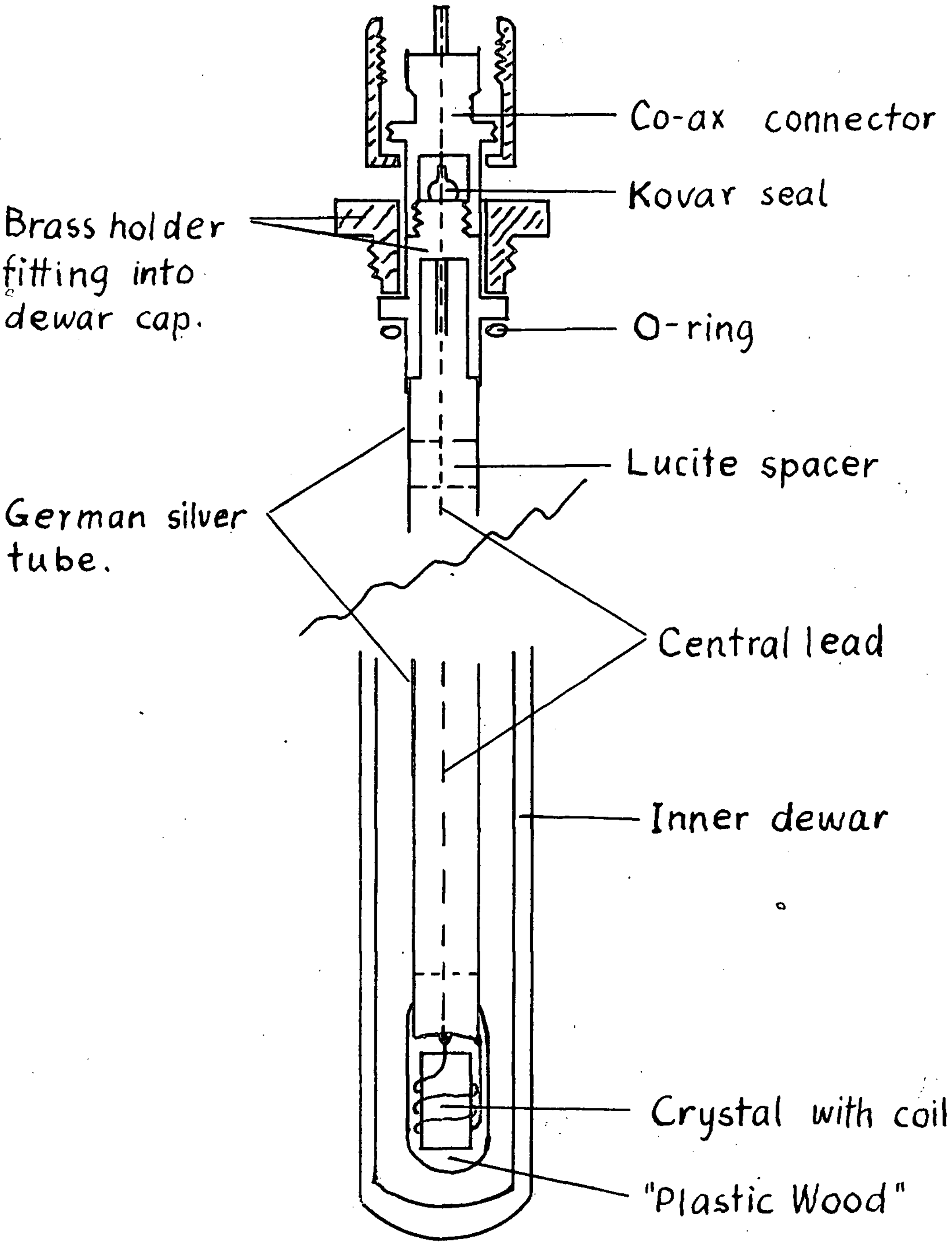

Fig. 5. Arrangement of crystal mount.

to follow page 14

orientation of the crystal cylinder in the plane of rotation of the magnet is not very critical, but the direction of the cylinder axis should be as nearly perpendicular to $\vec{H}_o$ as possible. A deviation of this axis from the ideal position may introduce spurious lines in the resonance spectrum. It was estimated that the cylinder axis was vertical to within about two degrees.

The cryostat was a common double dewar system. The supporting frame of the dewar cap was provided with set screws so that the German silver tube could be adjusted to be vertical and hence the cylinder axis (a- or b-axis of the crystal) was always perpendicular to the field $\vec{H}_o$ (the direction of $\vec{H}_o$ is adjusted to be horizontal). Thus $\vec{H}_o$ and $\vec{H}_1$ are always perpendicular to each other.

Temperatures lower than the boiling point of helium are obtained by pumping on the helium vapour. The lowest temperature obtained was about 1.52°K. The inner dewar has a capacity of about two liters and without pumping kept liquid helium for approximately twelve hours. The temperature is controlled by regulating the pumping speed and it is measured by observing the vapour pressure with a meniscus type cathetometer.

A pair of coils are mounted on the magnet pole pieces and are supplied from a Williamson type power amplifier. The sweep frequency is provided by an audio-oscillator which feeds into a phase shifting network. To this network are also connected the horizontal sweep of the oscilloscope and the reference voltage input of the phase sensitive detector, so that any phase relationship between the three units is possible. The oscilloscope is used mainly for adjustment purposes but may be used for actual measurements if only the frequency of the resonance lines is sought. When so used, the modulation amplitude is actually larger than the line width. To observe the derivative of the true line shape with a recording milliameter the modulation amplitude should be less than about 1/4 the line width. Observations at such low modulation amplitudes are made with the aid of a narrow band amplifier and the phase sensitive detector. To decrease the noise generated in the oscillator a fairly long time constant is inserted between phase sensitive detector and recorder reducing the noise band pass. This, however, requires that the time of sweeping through a signal be at least several times the time constant. In this way it is possible to run through a line spectrum continuously and record lines separated by many gauss on the same chart. To obtain the frequency at which resonance occurs, frequency markers are made on the chart at regular intervals by mixing the radiation from the oscillator with that of a B22-CA frequency meter and an ordinary radio receiver. The radio receiver and frequency meter are first set to zero-beat at the desired frequency. As the oscillator frequency passes through this zero-beat, one terminal of the recorder is momentarily grounded causing the needle suddenly to swing to one side.

The field H_o is determined by placing a water sample as close to the crystal as possible and measuring its resonance frequency with the aid of a second oscillating detector and the oscilloscope. The field is obtained from $\omega_o = \gamma H_o$, where γ is well known for protons in water. The magnet current was regulated with a highly stable Varian magnet current power supply, which kept the field constant throughout an entire helium run.

Chapter 4

Results

A. The $CoCl_2 \cdot 6H_2O$ Crystal.

Large crystals (3 x 1.5 x 1 cm) were grown from a saturated aqueous solution of $CoCl_2 \cdot 6H_2O$ by slowly evaporating it at room temperature. $CoCl_2 \cdot 6H_2O$ is of the monoclinic prismatic type. P. Groth[12] gives for a : b : c = 1.4788 : 1 : 0.9452 with = 122° 19'. Perfect cleavage occurs along the c $\{001\}$ face. X-ray studies of the single crystal were carried out by J. Miguno et al.[12]. These authors report two formula units per unit cell with space group determined as C_{2h}^3 - C^2/m. The atomic positions are given in the following table:

Kind of Atom	Position	x	y	z
Co	origin	0	0	0
Cl	4(i)	.278	0	.175
O_I	8(j)	.0288	$\pm$.221	.255
O_{II}	4(j)	.275	0	.700

A photograph of a three-dimensional model of the crystal structure is shown in figure 6.

According to the authors of reference 12, the two Cl^- ions and four water molecules are arranged octahedrally about the Co^{++} ions to form the group $CoCl_2 \cdot 4H_2O$, and the other two waters of the formula unit are located at somewhat greater distances from the cobalt ions. These shall be termed "relatively free" waters. Hydrogen bonds of the type $O_I \cdots H - O_{II} - H \cdots O_I$ and $O_I \cdots H \cdots Cl$ seem to form the group linkages in the plane parallel to (001), which would lead to the perfect cleavage along (001) as reported by P. Groth[11].

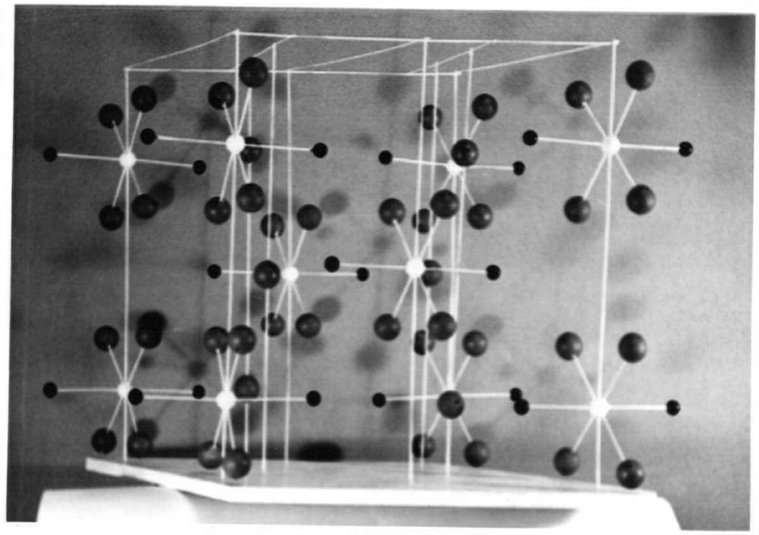

Figure 6. Photograph of three-dimensional model of crystal-structure of $CoCl_2 \cdot 6H_2O$.

White: Co^{++} ions

Small Black: Cl^- ions

Large Black: H_2O molecules.

to follow page 19

B. Discussions of Experimental Observations.

i. Introduction.

A complete analysis of the magnetic behaviour of $CoCl_2 \cdot 6H_2O$ is beyond the scope of this thesis. The work reported here is a preliminary survey of the proton resonance in $CoCl_2 \cdot 6H_2O$ at various temperatures. It is hoped that the results obtained will serve as a guide for more detailed investigations planned for the near future. These shall be a continuation and extension of the work reported here.

The experimental results fall into three groups: (a) measurements in the paramagnetic state, (b) observation of the phase transition, and (c) partially completed measurements in the antiferromagnetic state.

In making the measurements the crystal was kept fixed while the orientation of $\vec{H}_o$ was changed by rotating the magnet. In one set of measurements $\vec{H}_o$ was oriented in the a-c plane of the crystal, while in another set it was in the plane perpendicular to the a-axis. In the subsequent discussion zero angle shall refer to $\vec{H}_o$ perpendicular to the a-axis for the a-c rotation and to $\vec{H}_o$ parallel to the a-c plane for the rotation in the plane perpendicular to the a-axis.

A recording of the spectrum at 78°K with H_o in the a-c plane and at 160° is shown in figure 7. The corresponding spectrum at 4.2°K is shown in figure 8. Similar recordings

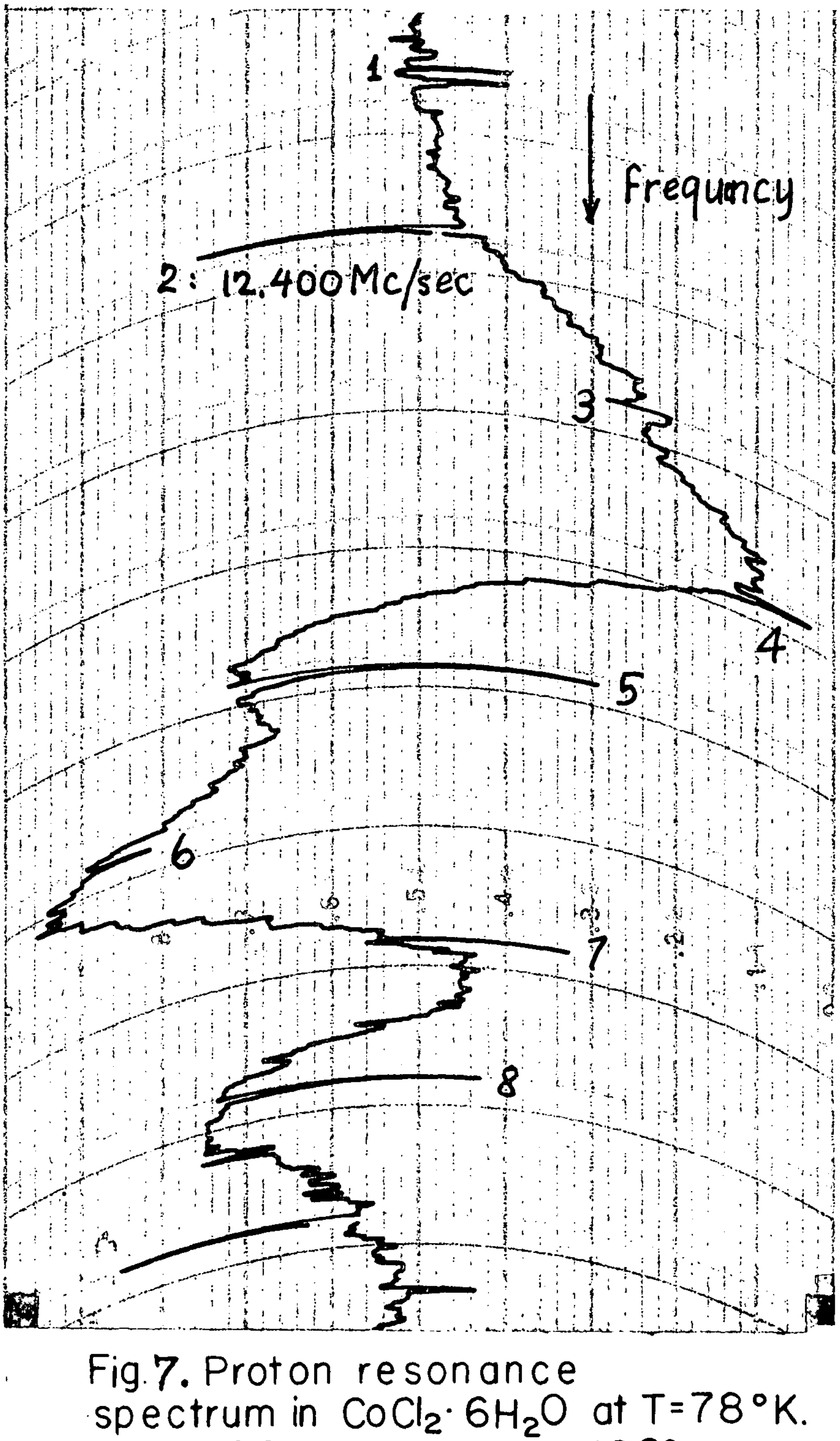

Fig. 7. Proton resonance spectrum in $CoCl_2 \cdot 6H_2O$ at T=78°K. H_0=3020 gauss. H_0 at 160° and rotating in a-c plane. Freq. marked in 20Kc/sec. steps.

to follow page 20

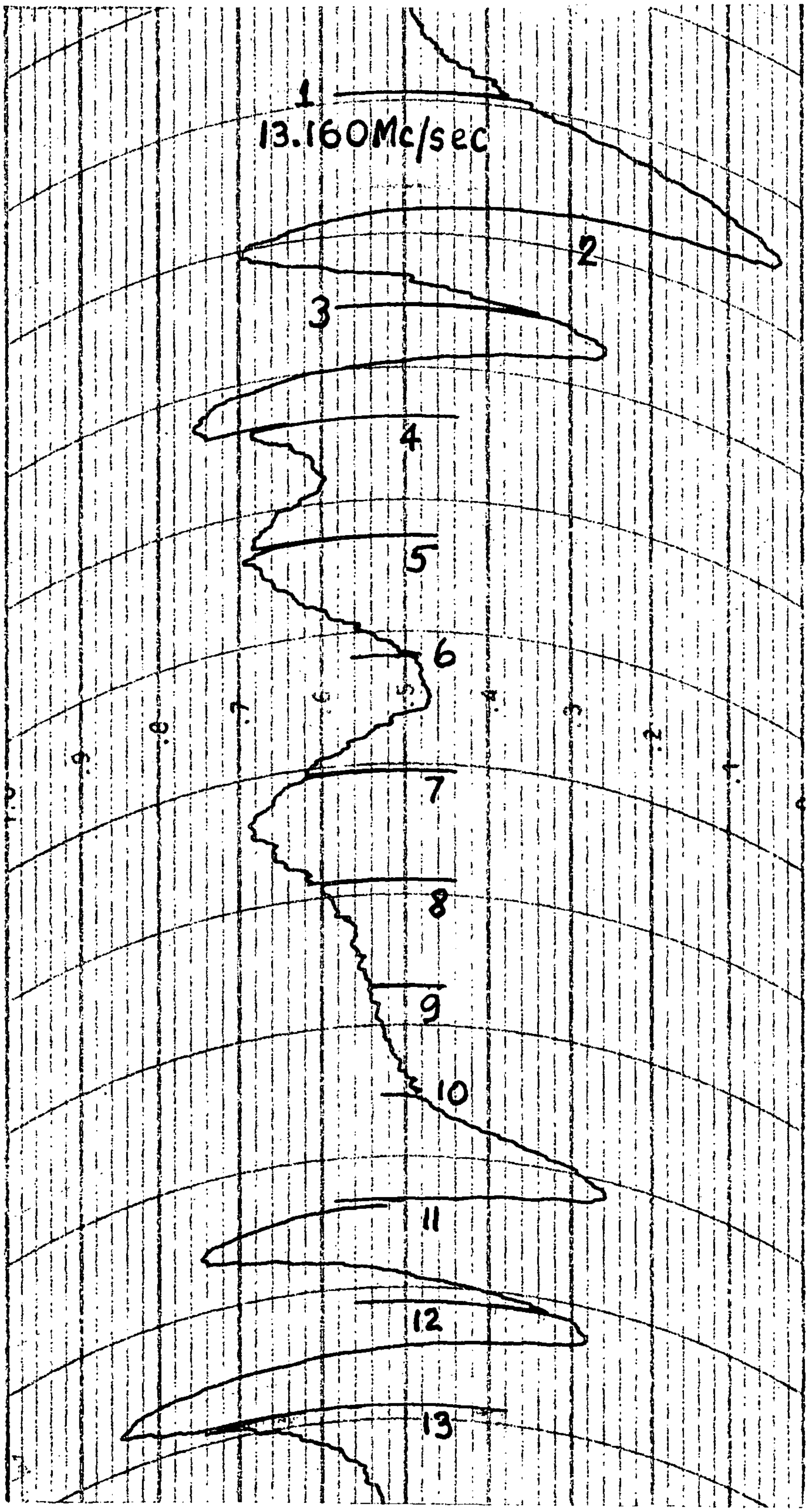

Fig.8. Same data as in fig.8.
T= 4.2°K. Freq. in 40 Kc/sec. steps.

to follow page 20

were obtained in each case for angular orientations between 0 and 180 degrees at 10 degree intervals. The results of the measurements of the angular dependence of the resonance line positions are shown in figures 10, 11, and 12. These correspond to rotations with H_o in the plane perpendicular to the a-axis at 78°K, and to rotations with H_o in the a-c plane at 78°K and 4.2°K respectively. The positions of the lines are given in the frequency scale. Each crystal position in these figures corresponds to a chart of the types in figures 7 and 8. The positions of the proton lines correspond to maxima in the absorption spectra and hence to zeros in their derivatives. Since most of the lines overlap the absorption curve will also contain minima, but only the 1st, 3rd, 5th, etc., zeros in the derivative curves represent proton lines (see figure 9). Due to this overlapping of neighbouring lines the observed maxima are slightly shifted from their true positions. No corrections have been made for such shifts. Each point in the graphs of figures 10, 11, and 12 corresponds to such a proton line. In each of these figures the solid vertical line represents the frequency of the protons in water (from which H_o is calculated) and shall subsequently be termed the "free proton" resonance frequency.

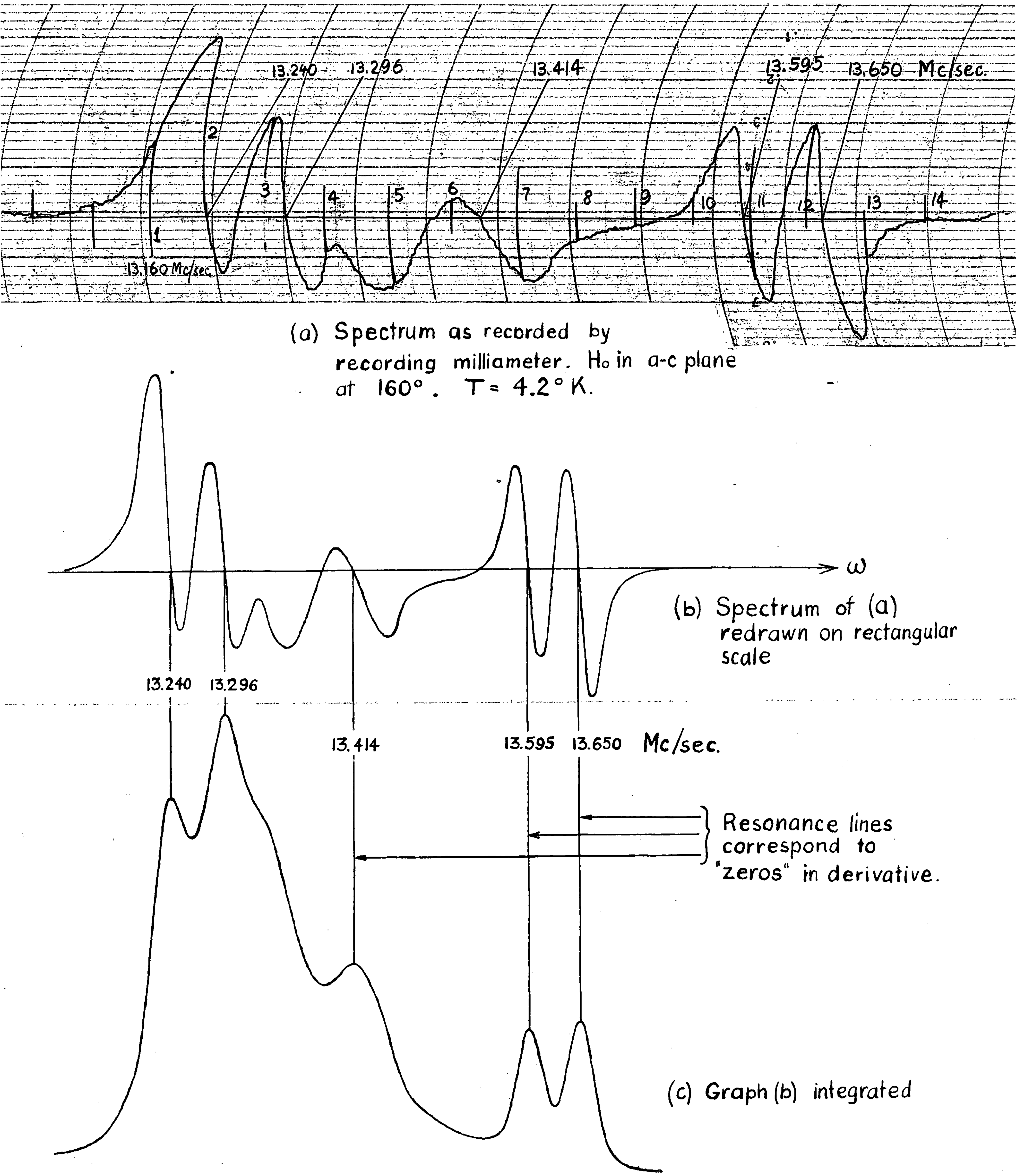

Fig. 9. Derivative of resonance line and actual line obtained by integrating (b) graphically.

to follow page 21

ii. Measurements in the Paramagnetic State.

The proton magnetic resonance spectrum was studied in single crystals of $CoCl_2 \cdot 6H_2O$ in a field H_o of about 3100 gauss. The maximum number of 24 lines predicted by theory was never observed. In the paramagnetic region two complete rotations were made at 78°K, one with $\vec{H}_o$ in the plane perpendicular to the a-axis, the other with $\vec{H}_o$ in the a-c plane. At 4.2°K one complete rotation was made with $\vec{H}_o$ in the a-c plane. The crystal remained fixed in space at all times, while the magnet was rotated about it in 10 degree intervals.

From each of these graphs we can see directly that the spectra repeat themselves after a 180-degree rotation of $\vec{H}_o$. Several checks were made at angles between 180 and 360 degrees, and these confirmed the 180-degree symmetry; consistent with paramagnetic measurements. This repetition of the resonance spectrum after a 180-degree rotation is due to the 180-degree periodicity of $(3\cos^2\theta-1)$.

(a) H_o in the Plane Perpendicular to the a-axis.

Figure 10 represents the only rotation with H_o in the plane perpendicular to the a-axis. A maximum number of three lines was observed, and they all overlapped strongly. It is thus impossible to follow any individual line through the whole rotation. Figure 10 exhibits a general symmetry about the b-axis. This indicates that the protons are situated symmetri-

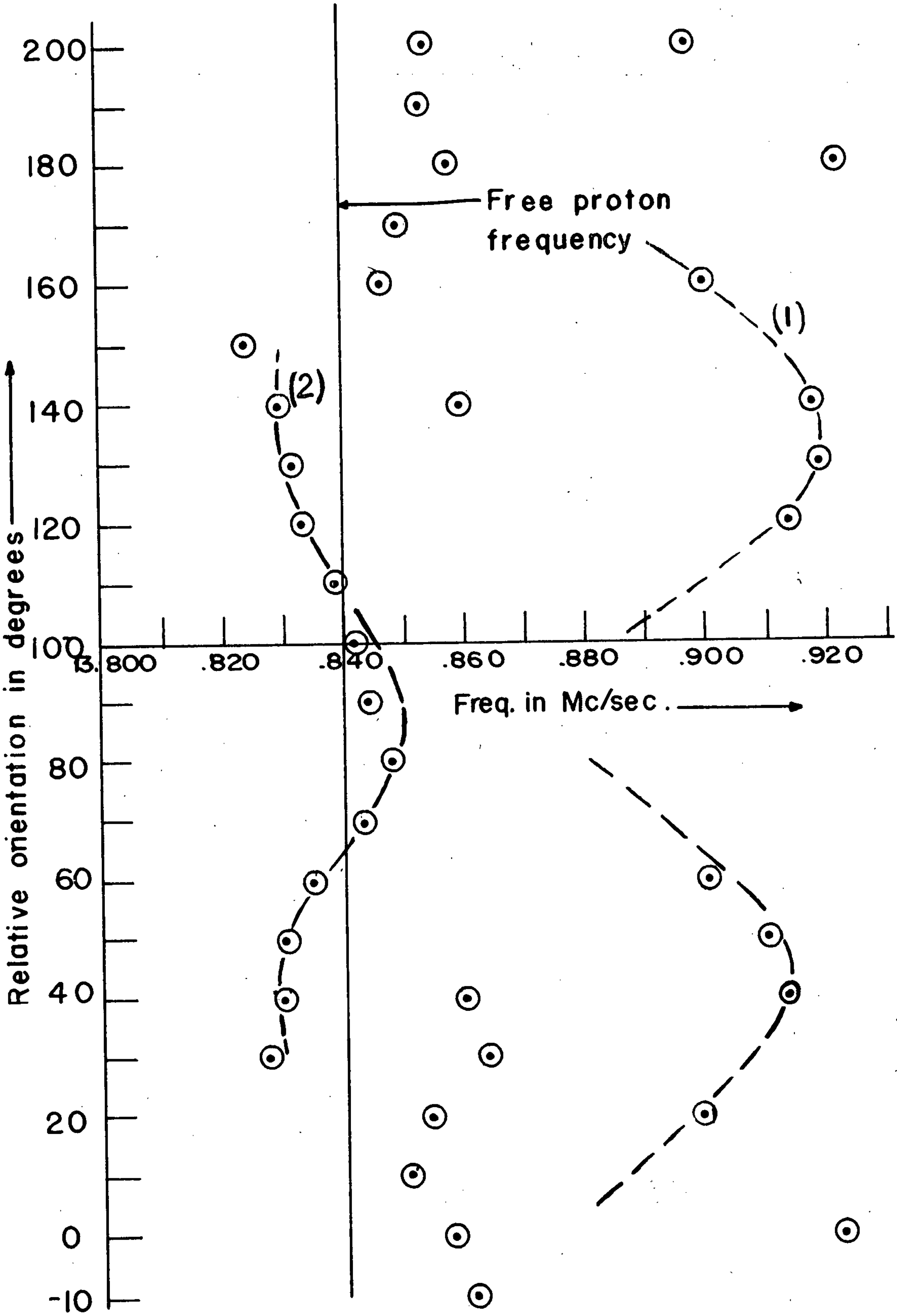

Fig. 10. Paramagnetic $CoCl_2 \cdot 6H_2O$ at 78°K
H_o rotating in plane perpendicular to a-axis

to follow page 22

cally with respect to the b-axis which is consistent with the crystal structure.

When H_o is parallel to the b-axis, all the lines occur above the free proton frequency. In this position the local field produced by the central cobalt ion in an octahedron is the same at all four surrounding oxygens O_I, and is in the same direction as $\vec{H}_o$ (the crystal structure reveals this (see figure 13a); and the g-factor of Co is positive). Therefore, if we disregard the relatively free waters and the neighbouring octahedra, the protons of the isolated octahedron should have a resonance frequency greater than the free proton frequency at this crystal position. The minimum and maximum resonance frequencies occur simultaneously at 45° on either side of the b-axis. When $\vec{H}_o$ is in this position the local field is almost in the same direction as $\vec{H}_o$ for two of the four waters, and opposite to $\vec{H}_o$ for the other two (see figure 13b), giving rise to resonance lines above and below the free proton line respectively as exhibited by figure 10. The points in figure 10 not falling on curves (1) or (2) may then be attributed to the relatively free waters.

It is of interest to examine some aspects of figure 10 quantitatively, since the plane perpendicular to the a-axis is within about 20 degrees of the reflection plane of the octahedron. For the angle 45°, $\vec{H}_o$ is almost parallel to the vector joining the central cobalt ion with two of the O_I atoms (actually, $\cos\theta = 0.97$ if θ is the angle between $\vec{H}_0$ and the vector joining the oxygen atoms and the cobalt ion), and exactly perpendicular to the vector from the cobalt ion to the other two O_I atoms in the octahedron. Taking the protons to be near the O_I atoms and noting that the field due to the cobalt ion is proportional to $(3\cos^2\theta-1)r^{-3}$, we expect the shifts of the proton frequencies due to these two groups of water molecules from the frequency corresponding to the <u>average total</u> internal field to be in the ratio $\frac{3\cos^2\theta}{-1}$ or $\frac{1.8}{-1}$. Clearly, in order that this be so, the <u>average</u> internal field must be taken to correspond to a proton resonance frequency approximately 19 Kc higher than the free proton value (see figure 10). We attribute this to the contribution of $(4\pi - N)M$ to the average field discussed at the end of chapter 2.

Since $\vec{H}_0$ was applied perpendicular to the cylinder-axis of our sample which is roughly a cylinder of length 1.6 times the diameter, N is approximately equal to 1.6π[8]. Assuming that $M \simeq \frac{CH_0}{T}$, where C is the Curie constant for our crystal and $T \simeq 78°K$, we calculate $C \simeq 0.014$.

The Curie constant is given by

$$C = \frac{N\, g^2 \beta^2\, S(S+1)}{3\, k}$$

where N is the number of paramagnetic ions per cm^3, g, β, and

S have been defined in chapter 2, and k is Boltzman's constant. Putting $g \simeq 4$ [13] and guessing that $S = \frac{1}{2}$, we obtain $C \approx 0.016$.

The close agreement of these two calculations of C is probably fortuitous, but it probably also indicates that our general interpretation is correct.

It will now be interesting in future studies to measure the temperature dependence of $\vec{M}$ by this method, and with the same geometry measure the temperature dependence of the maximum splitting of the lines. The first is proportional to the "space averaged" magnetization per unit volume while the second should be proportional to the time average magnetic moment of an individual cobalt ion. It would be surprising if they did not have the same temperature dependence. Nevertheless, an experimental check is of interest with respect to some fundamental ideas concerning internal magnetic fields. In the next section concerning the rotation of $\vec{H}_o$ in the a-c plane approximate verification of the above ideas is observed, since there we also have data in the paramagnetic state at liquid helium temperatures.

(b) $\vec{H}_o$ in the a-c plane.

Figure 11 represents the rotation with $\vec{H}_o$ in the a-c plane at 78°K and figure 12 the same rotation at 4.2°K. In figure 11 the number of lines is again small and the lines are never completely resolved, so that line identification is

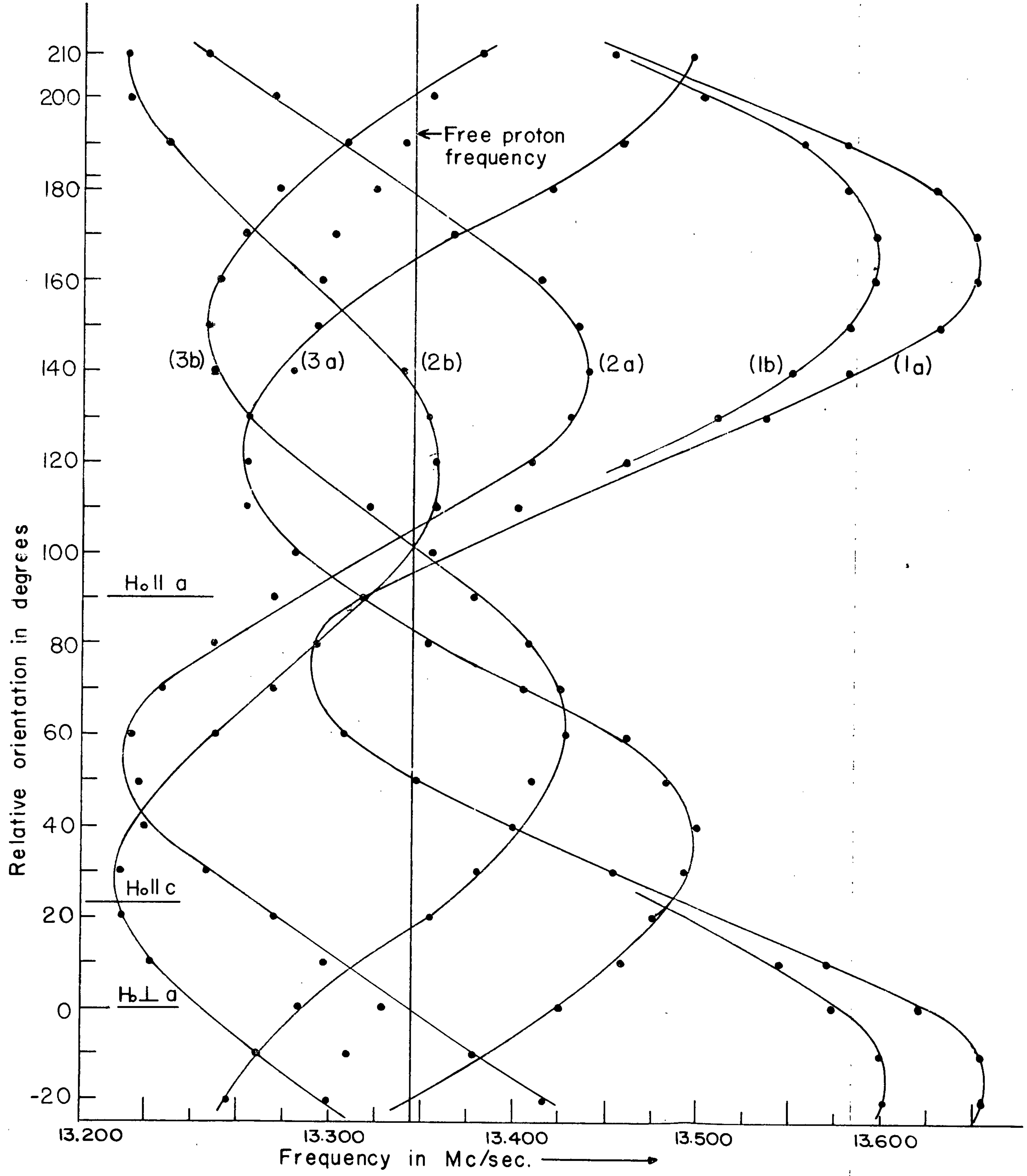

Fig. 12. Paramagnetic $CoCl_2 \cdot 6H_2O$ at 4.2° K. H_0 rotating in a-c plane. H_0 = 3.165 Kgauss.

to follow page 25

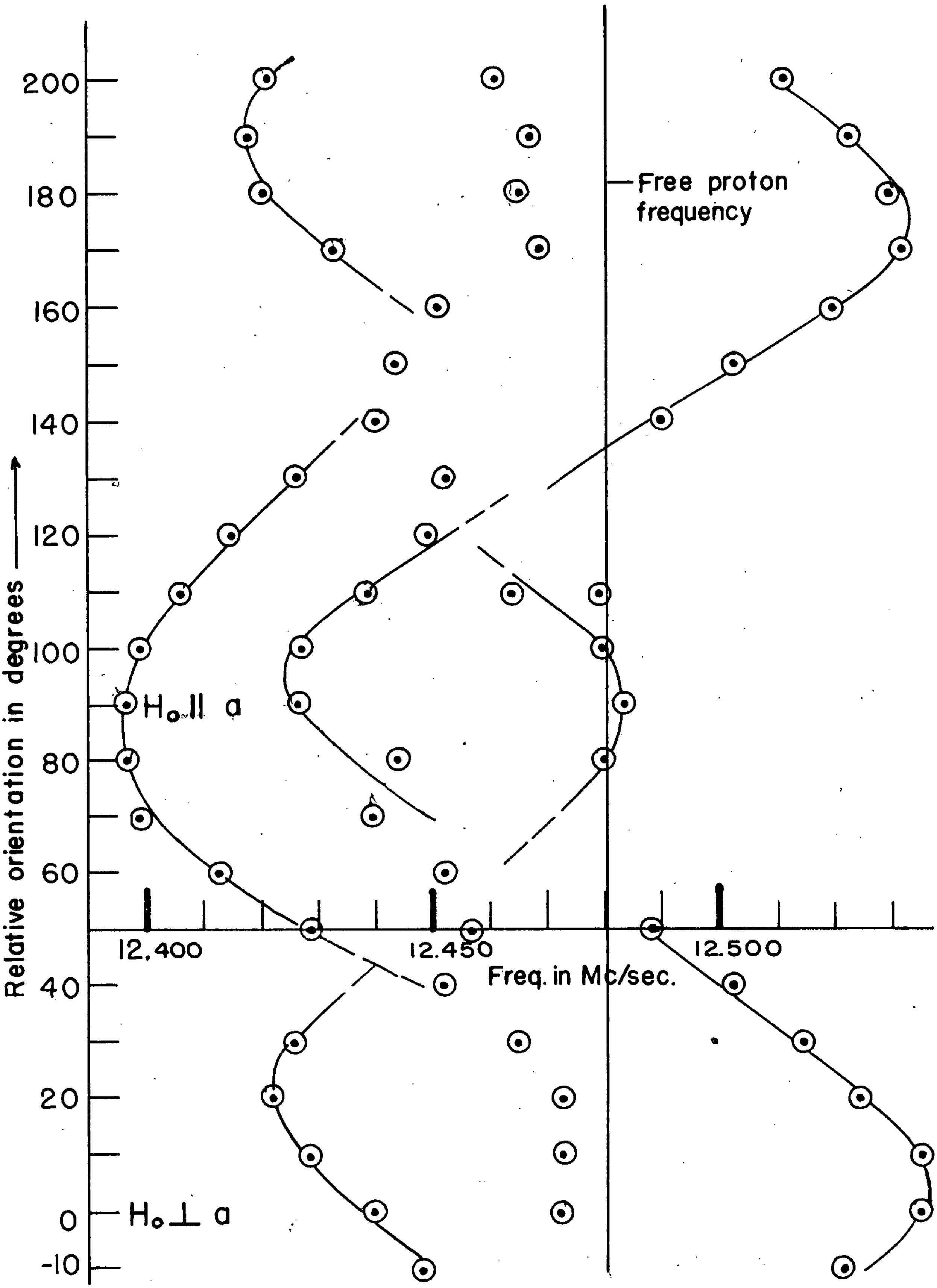

Fig. 11. Paramagnetic $CoCl_2 \cdot 6H_2O$ at 78° K.
H_o in a-c plane

to follow page 25

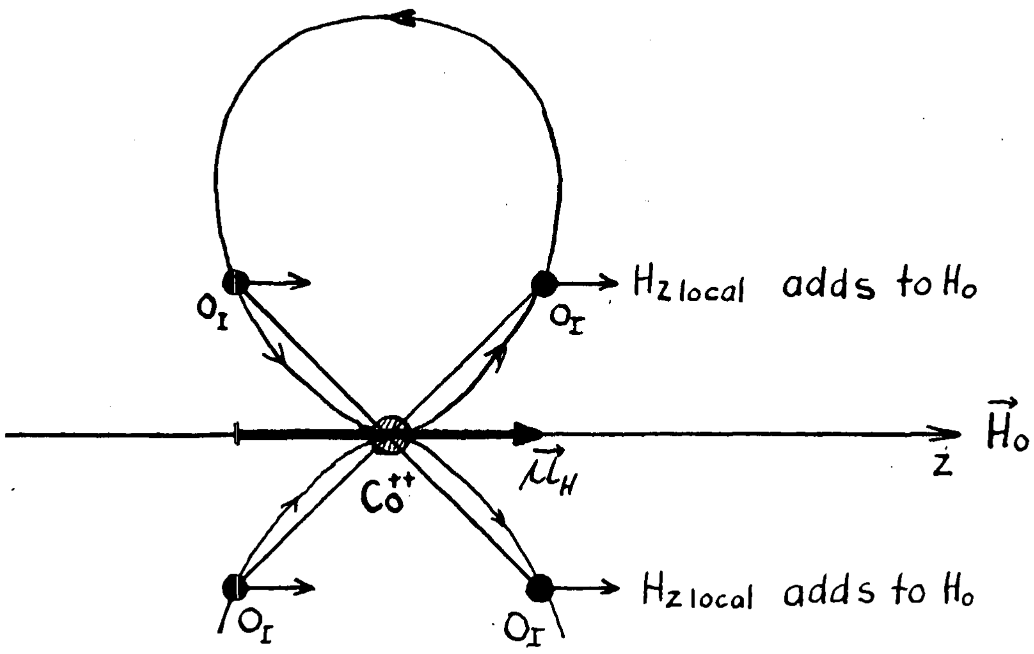

(a)

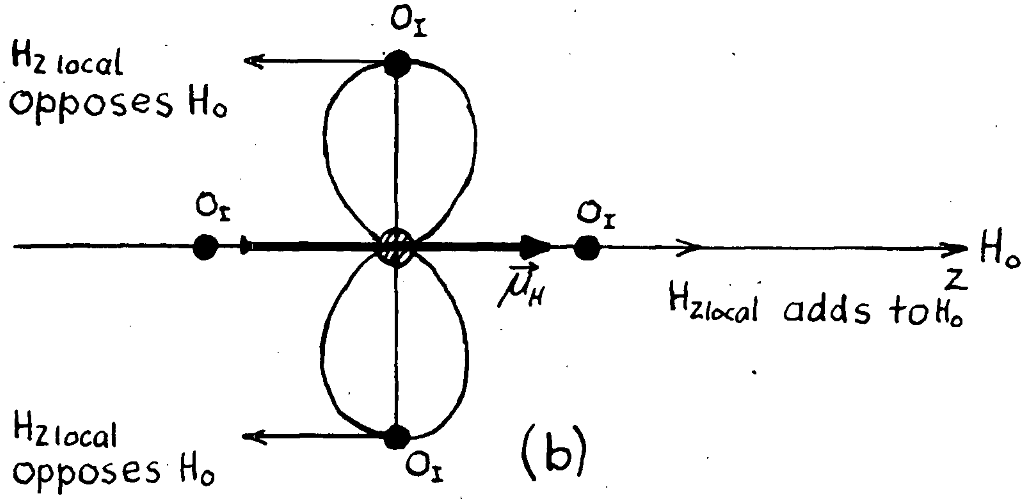

(b)

Fig. 13. Field pattern of a dipole.

to follow page 25

difficult.

Again the spectra are repeated after a 180-degree rotation due to the periodicity of $(3\cos^2\theta-1)$, as explained in the previous section. Comparing figures 11 and 12 we can recognize a general similarity in the two plots. In figure 11 the maximum frequencies occur at 0 degrees and 180 degrees, whereas in figure 12 they occur at -19 degrees and 161 degrees. At these orientations H_o is in the plane of the four oxygens O_I forming the reflection plane of the octahedron, and maximum frequencies are expected. However, these maximum frequencies should occur at the same crystal orientations regardless of temperature. Since different crystals were used for these rotations, the above discrepancy is probably due to faulty alignment of the sample for the rotation at 78°K. There must also be a slight misalignment of this sample relative to figure 10, since the spectrum at 0 degrees in figure 11 does not quite agree with the 0-degree spectrum of figure 10.

In figure 11 the majority of lines occur at frequencies below the free proton frequency, whereas in figure 12 the majority of lines occur above the free proton line. The ratio of the maximum frequency below the free proton line to that above in figure 11 is about 85 : 55, whereas in figure 12 the same ratio is about 165 : 305. In other words, at the lower temperatures the whole system of lines is shifted to higher frequencies.

Since the time averaged magnetic moment of the cobalt ions is proportional to $\vec{H}_o$, the splitting caused by the cobalt ions should be a linear function of H_o. The separation of extreme lines was measured as a function of H_o at 78°K for H_o in the a-c plane and with 160 degrees orientation, and also for $\vec{H}_o$ in the plane perpendicular to the a-axis at 0 degrees orientation. The results are shown in figures 16 and 15 respectively. In both cases the splitting is found to be linear in H_o, but when extrapolated for $H_o = 0$ the splitting does not become zero. This is to be expected, since the proton-proton interaction is independent of the applied field. For H_o in the a-c plane the splitting extrapolates to about 83 Kc or 19 gauss, and for $\vec{H}_o$ in the plane perpendicular to the a-axis it extrapolates to about 53.5 Kc or 12 gauss. The second of these values is almost exactly the usual proton-proton splitting in waters of hydration. The first value is somewhat high to represent pure proton-proton interactions, but since we do not know the relative amplitudes of the quantities a and b in formula 6, the slope of the line in figure 15 may actually change as H_o approaches zero.

In view of the above results the ideas put forward at the end of the last section concerning the rotation in the plane perpendicular to the a-axis can now be checked roughly.

For the angle -19° in this rotation $\vec{H}_o$ is in the reflection plane of the octahedron and for the angle 71° $\vec{H}_o$ is

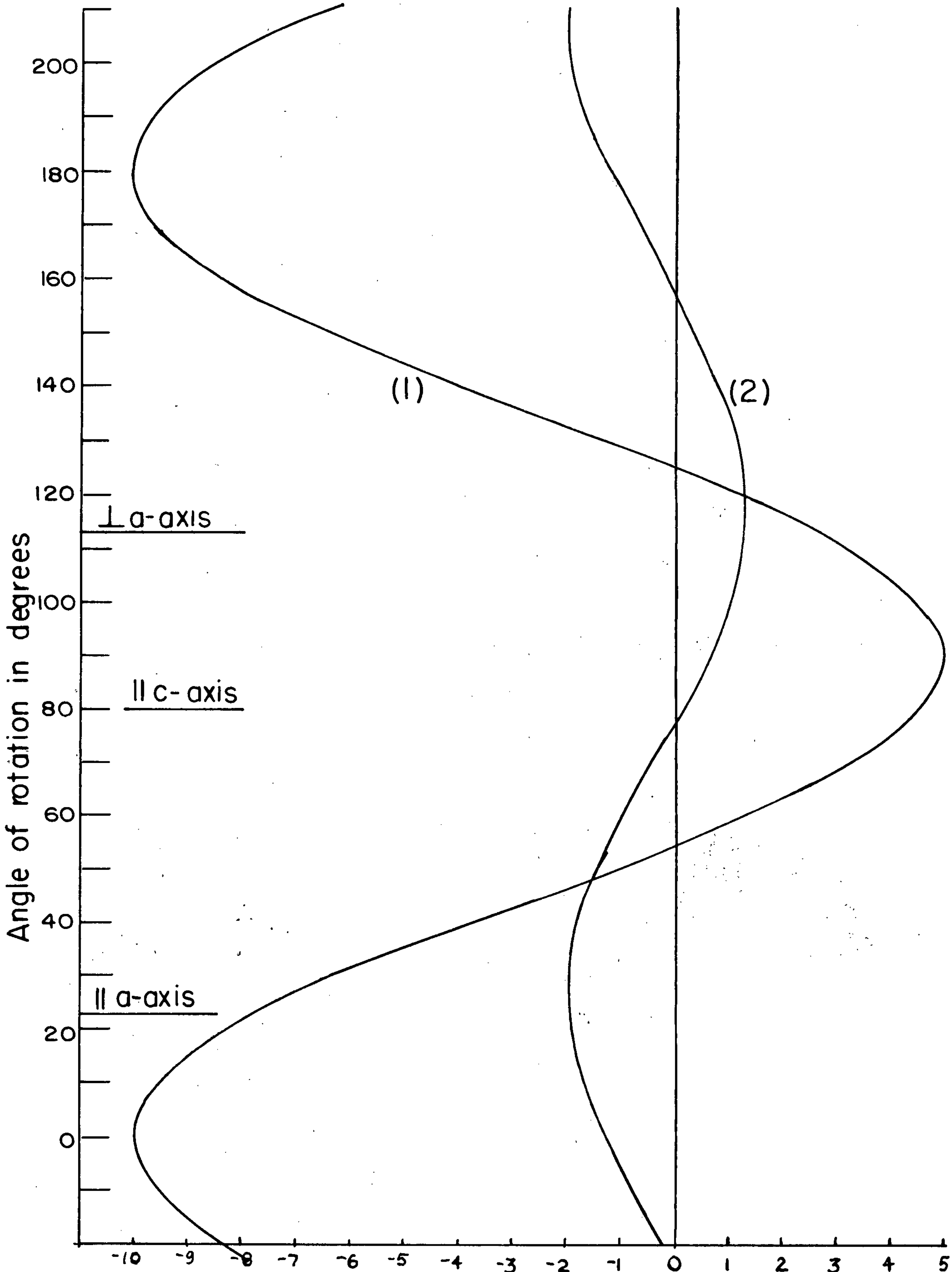

Fig. 14. See text.

to follow page 27

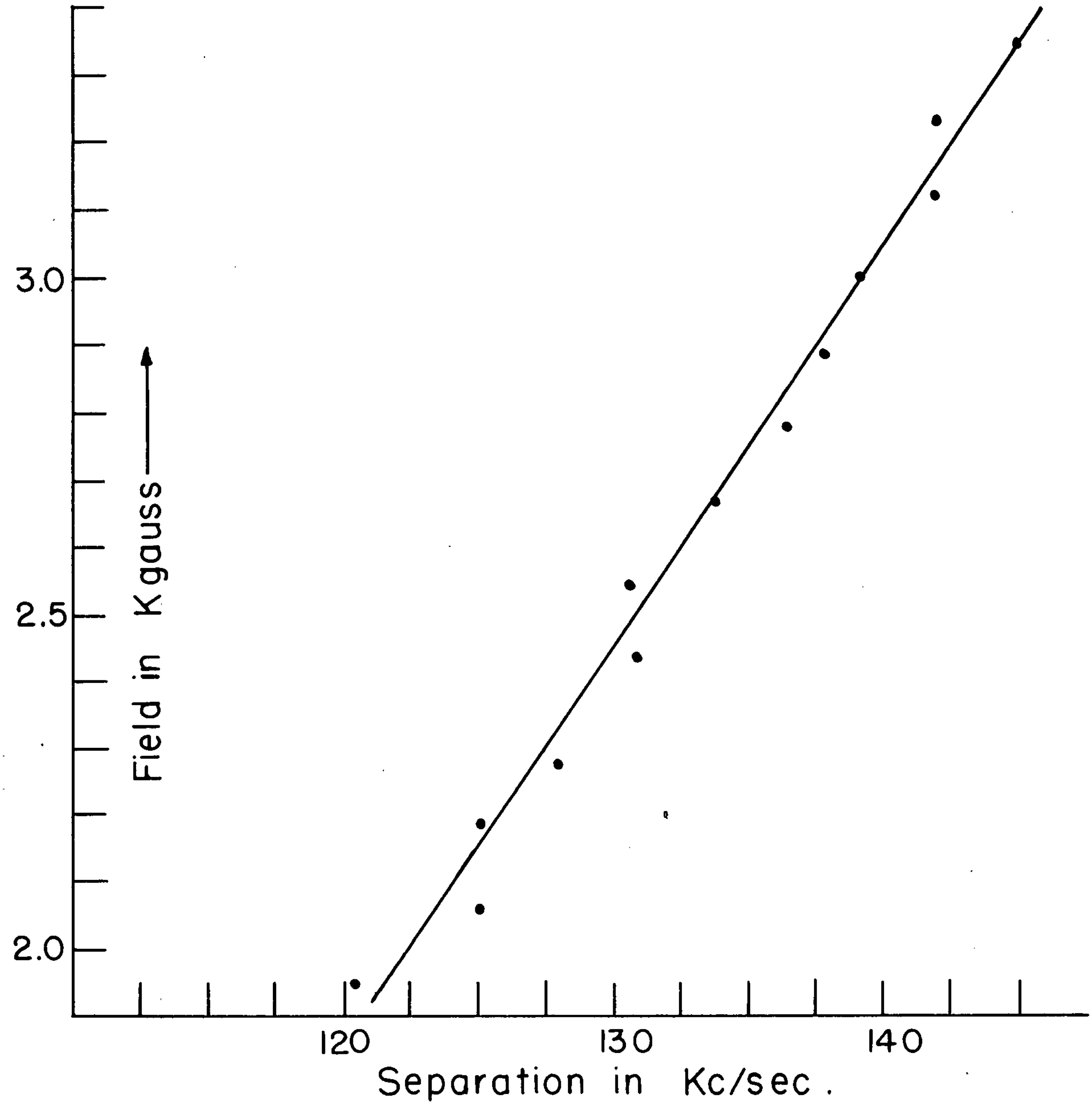

Fig. 16. Same as fig. 15. H_o at 160°
in a-c plane. T = 78 °K

to follow page 27

perpendicular to this plane. Again, taking the protons to be near the O_I atoms, <u>all</u> the protons associated with the O_I atoms are magnetically equivalent for the a-c rotation. Calculating the position of this line as a function of orientation of $\vec{H}_o$ in the a-c plane, we obtain curve (1) of figure 14. The extreme positions of the line above and below the average field are in the ratio of 1 : 2 respectively. This means that the average internal field in figure 11 should be taken to correspond to a proton resonance approximately 20 Kc higher than the free proton value. Within experimental error this is in agreement with the results for the rotation with $\vec{H}_o$ in the plane perpendicular to the a-axis. The extreme frequencies in curve (1) of figure 11 are about 12,427 Mc/sec. and 12,536 Mc/sec. which comes to a difference of 109 Kc. For the rotation at 4.2°K, considering curve (1a) in figure 12, the average field should be taken to correspond to a proton frequency about 197 Kc higher than the free proton frequency. The extreme frequencies for line 1a in this figure are about 13,183 Mc/sec. and 13,657 Mc/sec.; a difference of 372 Kc. Therefore

$$\frac{M\,(4.2°K)}{M\,(77.3°K)} \simeq \frac{197}{20} \simeq 10$$

and

$$\frac{\mu\,(4.2°K)}{\mu\,(77.3°K)} \simeq \frac{372 - 83}{109 - 83} \simeq 11$$

From these results we see that the "space averaged" magnetization $\vec{M}$ and the average value of the individual cobalt moment $\langle\vec{\mu}\rangle$ have the same temperature dependence within experimental accuracy. The dependence should not be expected to follow a simple Curie law.

Usually one can approximate the temperature dependence of magnetic susceptibilities by a Curie-Weiss law. If we assume that $\vec{M}$ and $\langle\vec{\mu}\rangle$ are proportional to $\frac{1}{T+\theta}$, where θ is the Curie temperature of the substance, then our results give approximately

$$\frac{78 + \theta}{4 + \theta} \simeq 10.5 \quad \text{or} \quad \theta \simeq 3.4°\text{K}$$

As described later, we have measured the Neel temperature of this substance to be approximately $T_N \simeq 2.28°$K. Since θ is normally greater than T_N, this result seems reasonable. It should be emphasized, however, that we have not tried to correct for the shift in the position of the lines due to overlap.

With well resolved lines and the proton positions known, the ratio of extreme frequencies for a particular line below and above zero shift due to $(3\cos^2\theta-1)r^{-3}$ could be obtained. In such a case the above ideas would, in fact, provide a method for measuring the average magnetization $\vec{M}$.

According to theory the six different water molecules of hydration in $CoCl_2 \cdot 6H_2O$ should lead to 24 lines in six groups of four. Each group of four should consist of two pairs, the centers of which are separated by a distance 2b (see formula 5), and the separation between these two lines is 4 d. They should be of equal intensity (see formula 7). However, experiments on $CoCl_2 \cdot 6H_2O$ never give 24 lines in a field of 3 K gauss. Thus, it may be concluded that certain lines overlap even at liquid helium temperatures. At 4.2°K a system of six lines consisting of three pairs is observed.

One of the major goals in this work is to find the positions of the protons in the unit cell. Since these are not yet known, we cannot give theoretical curves of the type of figure 12. However, an angular dependence of the form of figure 14 is obtained if we make the following assumptions: (i) disregard the two relatively free water molecules, (ii) assume that only the cobalt at the centre of the octahedron influences the four surrounding waters, (iii) neglect the effects of cobalt ions in neighbouring octahedra, and (iv) assume that the two protons in a water molecule do not interact and are situated at the O_I positions.

Curve 1 in figure 14 represents $H_z = (3\cos^2\theta-1)r^{-3} = (3\sin^2\beta\,\cos^2\alpha-1)r^{-3}$ as a function of α, where β is the angle between the Co^{++} - O_I vector and the projection of this line on the plane of rotation, and α is the angle between $\vec{H}_o$ and the plane of the O_I atoms. For the a-c rotation $\beta = \pi/4$ and r is, of course, a constant.

Choosing an arbitrary amplitude, this curve can be fitted exactly to curve 1a in figure 12 when the angles of rotation are chosen to coincide in the two figures. When $\vec{H}_o$ is perpendicular to the reflect ion plane of the octahedron, lines of lowest frequency are observed, since in this position the local field due to the central cobalt is opposite to the direction of $\vec{H}_o$ because cobalt has a positive g-factor (3 unpaired electrons in the 3d shell). When $\vec{H}_o$ is perpendicular to the C_4 axis of the octahedron, i.e. parallel to the reflection plane, lines of maximum frequency are observed. This is in agreement with figure 14.

In reality, of course, the two protons are not at the oxygen positions and they do interact, but the fact that curve 1 in figure 14 and curves 1a and 1b in figure 12 are almost exactly in phase means that one of the protons is located in the reflection plane of the octahedron. If we consider the octahedron as an isolated system, potential energy and symmetry considerations should cause the other proton also to be in this plane. But in the crystal one such octahedron is surrounded by many others, and the second proton in the waters may be twisted slightly out of this plane. Such a position would produce a pair of curves slightly out of phase with curves 1a and 1b in addition to having different frequencies. Curves 2a and 2b are out of phase by about 30° with curves 1a and 1b.

The splitting in the pair 1 and 2 is of the order of 10-15 gauss, which is the usual splitting in a water molecule due to proton-proton interaction. It may be, then, that the separation in pairs 1 and 2 is due to the proton dipole-dipole interaction. Curves 1a and 1b in figure 12 coalesce near $\alpha = 71°$ when $\vec{H}_o$ is perpendicular to the reflection plane of the octahedron. This implies that the proton-proton splitting in curve-pair 1 is zero at this position. Therefore, $(3\cos^2\theta_{12}-1) = 0$ in this orientation, where θ_{12} is the angle between the vector connecting the two protons and its projection on the plane of rotation of the magnet. If the splitting is truly zero, and more detailed studies may reveal that it is not, then the direction of the line connecting the two protons could be determined.

The splitting between the centres of pairs 1 and 2 is therefore assumed to be caused by the central cobalt. In this argument the effect of the neighbouring cobalts was neglected. Since the nearest cobalt-neighbours to any of the protons are about twice the distance of the central cobalt to any of its surrounding protons, their effect is reduced by a factor 8 at least due to the $\frac{1}{r^3}$ behaviour of a dipole field, and so should produce only a slight change in the curves of figure r.

Curve 2 in figure 14 represents the local field at the position of an O_{II} due to its four nearest cobalt neighbours drawn to the scale of curve 1. This curve, however, is not in phase with curve-pair 3 in figure 12, which merely indicates that the protons of the relatively free waters are not located at the O_{II} positions. The splitting in this pair of lines cannot definitely be accounted for. It is probably due to a proton-cobalt interaction, since it is too large for a proton-proton interaction (about 30 gauss), unless these water molecules are greatly distorted.

Quantitative results cannot be given at this time, since not sufficient data have been recorded. The work planned for the immediate future will incorporate these qualitative arguments, and it is hoped that it will be possible to establish the proton positions.

The first obvious extension of the work reported here is to repeat the measurements at much higher fields so that a better resolution is obtained. Probably more lines will then appear and definite identification should be possible. A study of the splitting between certain pairs of lines as a function of field at given positions should reveal which splittings are caused by proton-proton interactions and which are due to the cobalt ions.

It is also planned to perform double resonance experiments. With the aid of these it should be possible to study line shapes even if the lines normally still slightly overlap. Crystals containing different concentrations of D_2O should reveal some interesting phenomena, as it should be possible to eliminate certain proton lines and to observe the lower frequency deuteron resonance lines. With the results from these measurements and the completion of the observations in the antiferromagnetic state it should be possible to completely describe the magnetic behaviour of $CoCl_2 \cdot 6H_2O$.

iii. Transition Temperature Measurements.

T. Haseda and E. Kanda[14], and M. Leblanc[15] independently found that $CoCl_2 \cdot 6H_2O$ exhibits an antiferromagnetic behaviour below about 3°K. W.K. Robinson and S.A. Friedberg[16] observed a lambda-type anomaly in the specific heat of $CoCl_2 \cdot 6H_2O$ at 2.29°K and assumed this anomaly to be associated with a paramagnetic-antiferromagnetic phase transition. In this work the transition temperature was measured by observing the change in the proton spectrum.

Figure 17 shows the proton spectrum at 2.5°K with H_o at 160° in the a-c plane. The frequency of the oscillator was adjusted so that the recorder pen rode on the first maximum slope of the spectrum which corresponds to the first maximum in figure 17 as indicated. With the frequency held constant at this point, the temperature was slowly decreased. As a result the graph of figure 18 was obtained. The temperature check points are marked on the graph by small pips in the curve, and the corresponding temperatures are listed in this figure.

Figure 18 shows that the onset of the transition occurs at slightly above 2.28°K in agreement with the specific heat measurements by Robinson and Friedberg. At this temperature the line of the paramagnetic state disappears, but the change is not abrupt. The transition takes place over a temperature

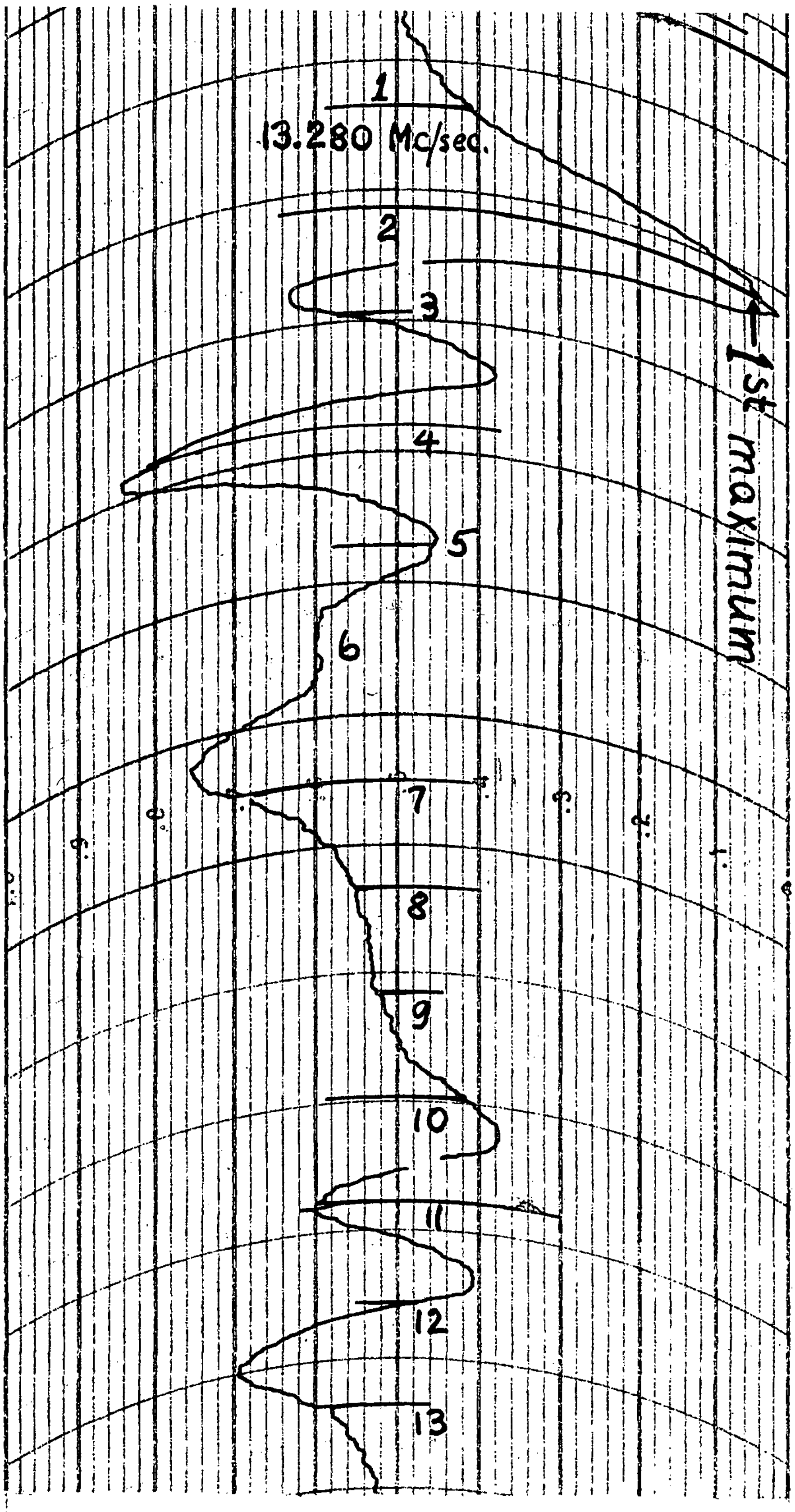

Fig. 17. Proton spectrum at
at T=2.5°K. H_o at 160° and in
a-c plane. Freq. in 40 Kc/sec. steps

to follow page 35

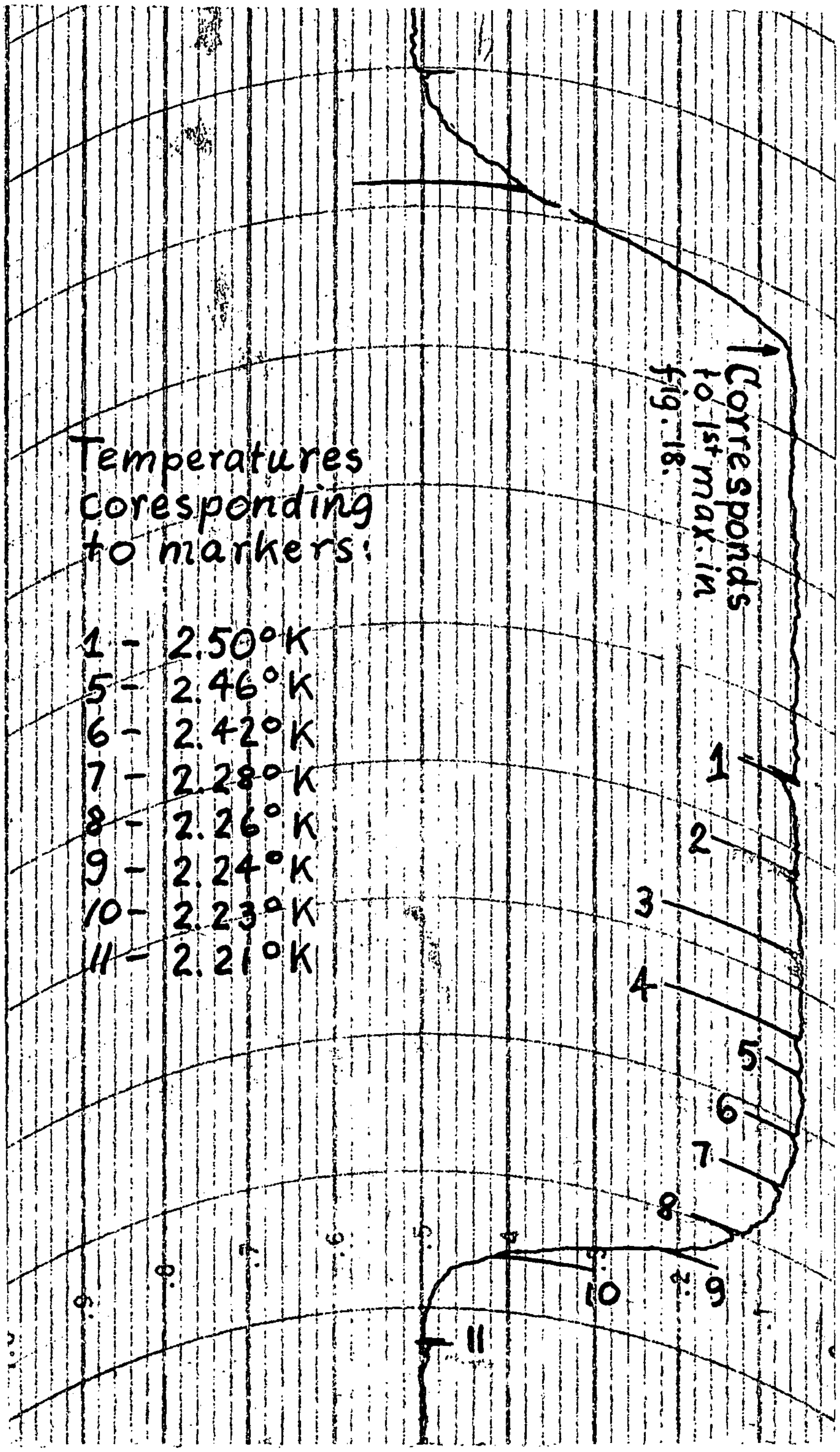

Fig. 18. Transition Temperature.

to follow page 35

range of about 0.07° (pips 7 to 11). This range is not caused by time effects in the recording system. Several such graphs were obtained with different rates of temperature change, and the range through which the transition takes place was about 0.07° in each case. The error in the temperature measurements may be as large as ±0.03°, but temperature differences could be measured to a much higher degree of accuracy. The fact that the transition is not sudden but takes place over a certain temperature spread indicates that short-range magnetic order effects are present.

It was possible to keep the temperature constant at any point, and several recordings of the spectrum were made with the transition partially completed. One such recording at 2.25°K is shown in figure 19. This spectrum still resembles that of figure 17 (recorded at 2.5°K), but a change is easily recognizable. Recordings at lower temperatures within the transition range further deviate from figure 17, until the transition to the anti-ferromagnetic state is complete. Figure 20 shows part of a spectrum at 2.21°K (just below the transition temperature). Other lines occur in this spectrum several Mc/sec. on either side of the part shown.

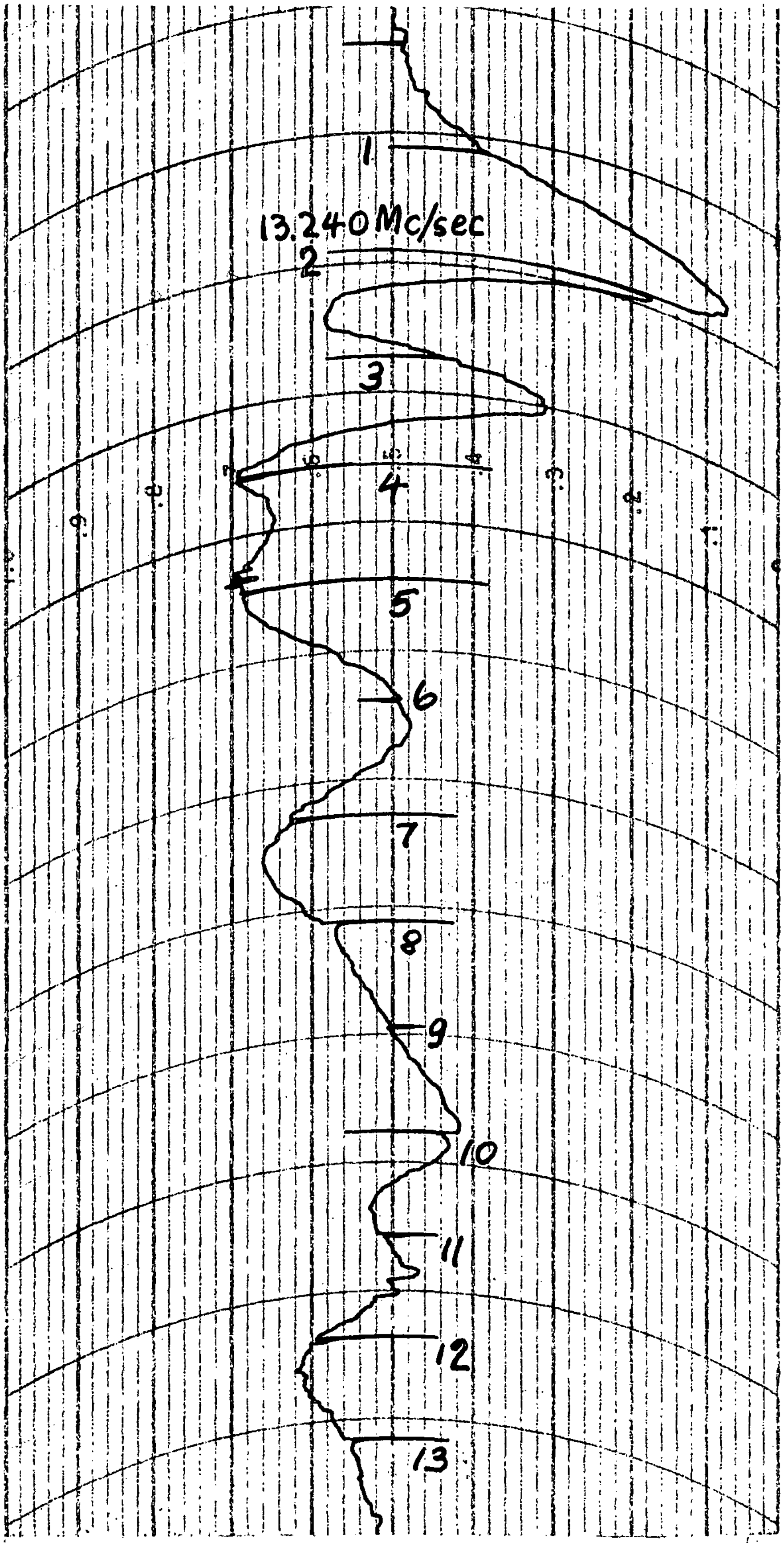

Fig. 19. Proton spectrum at T = 2.25° K. H_o at 160° and in a-c plane. Freq. in 40 Kc/sec. steps.

to follow page 36

iv. Measurements in the Antiferromagnetic State.

As stated before, $CoCl_2 \cdot 6H_2O$ becomes antiferromagnetic at about 2.28°K. Measurements in the antiferromagnetic state are only partially complete. These were carried out at 1.52°K in a field of 3100 gauss with $\vec{H}_o$ in the a-c plane. A recording of the spectrum with $\vec{H}_o$ at 20° is shown in figure 21. The results are shown in figure 22. Figure 22 is of the same type as figure 12, the angular orientation being the same in both graphs.

These results exhibit some features strikingly different from the measurements in the paramagnetic temperature region. The spectrum and the number of lines change essentially in passing from the paramagnetic to the antiferromagnetic region. Line shifts of 7.5 Mc/sec. have so far been recorded. Probably these will increase to about 15 Mc/sec. when the rotation is completed. The lines are well resolved and generally much broader (of the order of 120 Kc/sec. or about 28 gauss). Figure 21 shows a typical recording of the proton resonance at 1.52°K for a given orientation of $\vec{H}_o$. The data in figure 22 are derived from such recordings.

One striking and as yet unexplained feature in all recordings in the antiferromagnetic state is the very strong line approximately 30 Kc/sec. above the free proton frequency. This line is not affected by the orientation of $\vec{H}_o$ in the

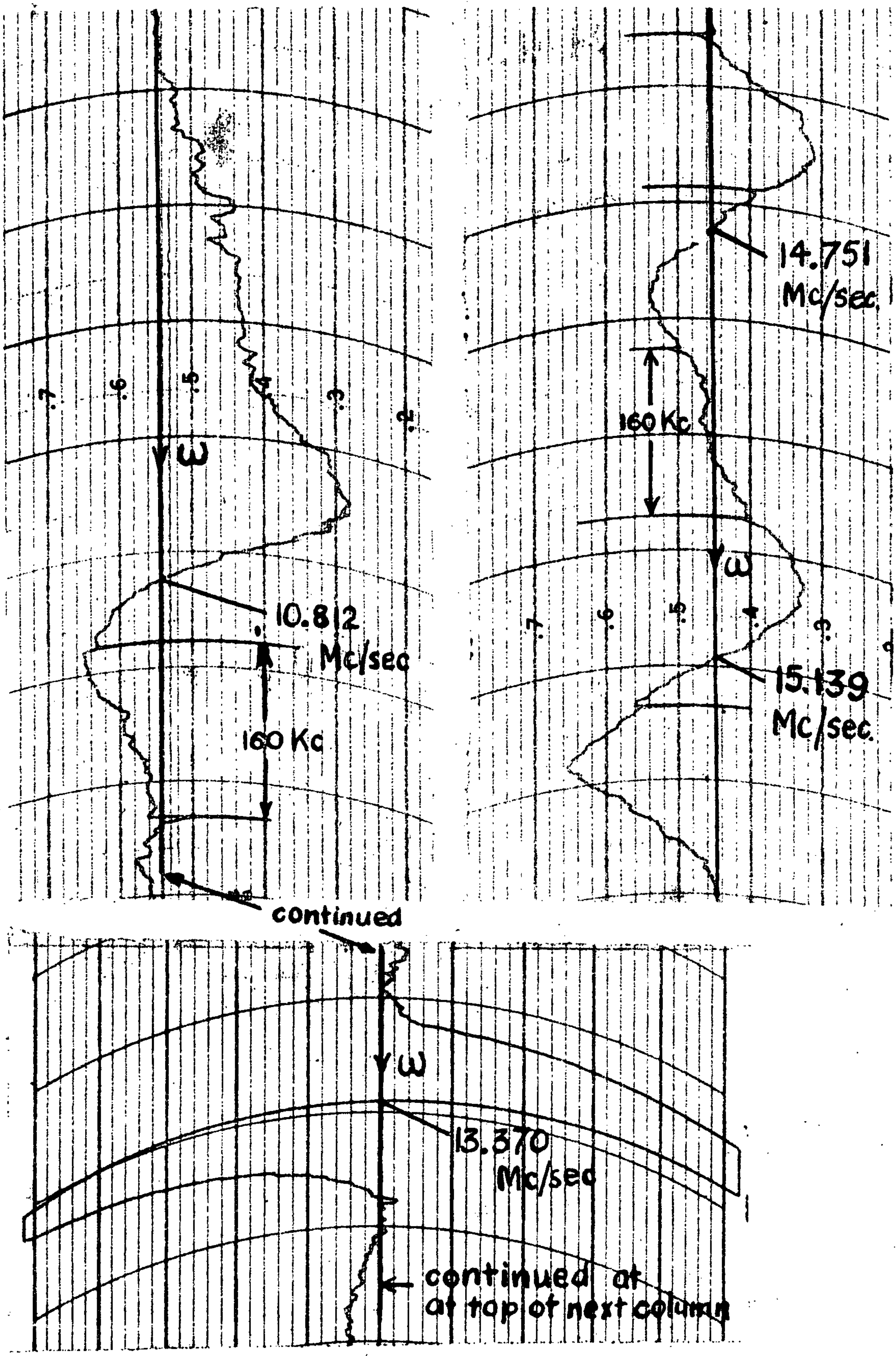

Fig. 21. Proton resonance spetrum in Anti-ferromagnetic state at 1.52°K. H_0 in a-c plane at 20°.

to follow page 37

a-c plane.

When the rotation in the antiferromagnetic state is completed, it appears that the spectrum will be symmetric only with respect to 360° rotation instead of 180° as in the paramagnetic state. This result is expected, since in the antiferromagnetic state the magnetic ions are oriented with respect to the crystal axes rather than the external magnetic field $\vec{H}_o$.

Bibliography

1. G.E. Pake, J. Chem. Phys. 16, 327 (1948).
2. N. Bloembergen, Physica 16, 95 (1950).
3. N.J. Poulis, Physica 17, 392 (1951).
4. N.J. Poulis, Physica 18, 201 (1952).
5. J.H. Van Vleck, Phys. Rev. 74, 1168 (1948).
6. N. Bloembergen, E.M. Purcell, and R.V. Pound, Phys. Rev. 73, 679 (1948).
7. J.H. Van Vleck, J. Chem. Phys. 5, 320 (1937).
8. American Inst. of Physics Handbook, Chapter 5, p. 240.
9. D.G. Watkins, Ph.D. Thesis, Harvard University, Cambridge, Mass., U.S.A. (1952).
10. H.H. Waterman, Ph.D. Thesis, University of B.C. (1954).
11. P. Groth, Chemische Krystallographie, 1. Teil, p. 248, Wilhelm Enzelmann Verlag, Leipzig (1906).
12. J. Mizuno, K. Ukai, T. Sugawara, J. Phys. Soc. Japan 14, 383 (1959).
13. M. Date, J. Phys. Soc. Japan 14, 1244 (1959).
14. T. Haseda, E. Kanda, J. Phys. Soc. Japan 12, 1051 (1957).
15. M. Leblanc, Ph.D. Thesis, University of B.C. (1958).
16. W.K. Robinson, S.A. Friedberg, Tech. Report No. 5, Carnegie Inst. of Tech., Dept. of Physics (1959).